LICENTIATE THESIS

Computed Tomography of Sawlogs - Knot Detection and Sawing Optimization

Erik Johansson

LULEÅ UNIVERSITY OF TECHNOLOGY

Computed Tomography of Sawlogs – Knot Detection and Sawing Optimization

Erik Johansson

LULEÅ
UNIVERSITY
OF TECHNOLOGY

Wood Technology
Division of Wood Science and Engineering
Department of Engineering Sciences and Mathematics
Luleå University of Technology
Skellefteå, Sweden

Supervisors:

Johan Oja and Anders Grönlund

Licentiate Thesis
Department of Engineering Sciences and Mathematics
Luleå University of Technology

This thesis has been prepared using LaTeX

Copyright © Erik Johansson, 2013.
All rights reserved

Wood Technology
Division of Wood Science and Engineering
Department of Engineering Sciences and Mathematics
Luleå University of Technology
SE-931 87 Skellefteå, Sweden
Phone: +46(0)920 49 10 00

Author e-mail: erik.johansson@ltu.se

Printed by Universitetstryckeriet, Luleå 2013

ISSN: 1402-1757
ISBN 978-91-7439-716-1 (print)
ISBN 978-91-7439-717-8 (pdf)

Luleå 2013

www.ltu.se

Abstract

Branches on trees introduce defects on sawn timber called knots. By scanning sawlogs using computed tomography, knots can be detected and accounted for so that the sawing process can be optimized with respect to outgoing product value. How the optimization should be done differs depending on available sawing equipment and the production strategy of the sawmill. It is important to investigate interesting production strategies with computer simulations to obtain an approximation of the profitability for a sawmill if investing in a computed tomography scanner. Another important step in the optimization process is to automatically segment knots so that they can be used by a computer when optimizing.

This thesis presents an algorithm that automatically segments knots from computed tomography images of logs. The algorithm uses variable thresholds to segment knots on cylindrical shells of the computed tomography images. The knots are fitted to ellipses and matched between several cylindrical shells. The algorithm was tested on a variety of Scandinavian Scots pine (*Pinus sylvestris* L.) and Norway spruce (*Picea abies* (L.) Karst.) with a knot detection rate of 88-94 % and generating about 1 % falsely detected knots.

Knots are defects with high impact on boards that are graded with respect to their bending strength. Some sawmills specialize in the production of such boards and this thesis includes a simulation study of sawing Norway spruce (*Picea abies* (L.) Karst.) logs to optimize the outgoing board value for such a sawmill. The production strategy investigated in this thesis was scanning of sawlogs with computed tomography and optimizing the rotational positioning of the logs in the sawing process. This study showed a possible mean value increase of the sawn timber by 11 %.

There are additional degrees of freedom in log breakdown than rotational positioning, such as log spatial position, skew and which sawing pattern to use. If every possible combination of sawing parameters would

be simulated, enormous computational resources would be required. A study made in this thesis investigates the feasibility to use only parts of the knot information when optimizing log rotational position. This is done by projecting all knots to a plane perpendicular to the log lengthwise direction and filter out the least significant knots. The study showed a great challenge in this approach and the presented algorithm was insufficient in its present form to compete with alternatives that use full information of the knots.

Preface

The work of this thesis has been carried out at the Division of Wood Science and Engineering at Luleå University of Technology and SP Technical Research Institute of Sweden, Skellefteå. The research was funded by WoodWisdom-Net and VINNOVA through the project CT-Pro and by the European Union Objective 2. I appreciate the financial support that let me complete the work of this thesis.

I would like to thank all project partners within CT-Pro for valuable support and interesting discussions. My supervisors, Johan Oja and Anders Grönlund have with their experience and sharp minds helped me navigate though the first few years of my doctoral studies when my own thoughts have been puzzled. Thank you. I also want to thank SP Technical Research Institute of Sweden for giving me the opportunity for doing doctoral studies.

My gratitude also goes toward all family members, friends and coworkers who have been there for me when times have been tough. Finally, special thanks go to Malin. With you around, the world is a little more colorful. Therefore, the most colorful of pages, 53, is dedicated especially for you. Enjoy!

Skellefteå, August 2013

Erik Johansson

List of publications

This thesis is based on the following publications:

Paper I
Johansson, E., Johansson, D., Skog, J. and Fredriksson, M., 2013: Automated knot detection in computed tomography images of *Pinus sylvestris* L. and *Picea abies* (L.) Karst. using ellipse fitting in concentric surfaces. *Computers and Electronics in Agriculture*, 96, 238-245.

Paper II
Fredriksson, M., Johansson, E. and Berglund, A., 2013: Rotating *Pinus sylvestris* sawlogs by projecting knots from computed tomography images onto a plane. *Submitted to journal.*

Paper III
Berglund, A., Johansson, E. and Skog, J., 2013: Value optimized log rotation for strength graded boards using computed tomography. *Submitted to journal.*

Contents

Part I

Chapter 1

Introduction

One of the fundamental challenges in the sawmill industry is that the raw material, i.e. sawlogs, is round and that the market demands specific dimensions of square timber. This combined with differences between logs lead to raw material waste in the log breakdown process. To combat this, sawmills often utilize non-invasive three dimensional measurements of logs moments prior sawing. With use of optimization algorithms applied on computer models of the logs, the waste of raw material can be minimized.

To make matters more complex, the value recovery of a log not only depends on the volume of the sawn products, but also on quality grade of the products. By using only outer shape information of logs, important internal quality properties such as knot content and density cannot be accounted for when optimizing log rotational position. Discrete x-ray measurement techniques can be used to gather general information of those properties, but the measurement precision is low for knot geometry (Grundberg and Grönlund, 1998; Oja et al., 2001).

An x-ray technique with higher level of detail is computed tomography (CT), which yields detailed pictures of log interior composition. CT has been used extensively in research of wood related topics where scanning speed is not an issue. Nowadays, some scanners are fast enough to be used on-line at sawmills with feed speeds of more than two meters per second (Giudiceandrea et al., 2011).

To use such a scanner in practice, algorithms that automatically extracts information about interesting features are required. Knot content is a particular feature in logs that are important for board quality. An

example of the importance of knot content is a previous study on Scots pine (*Pinus sylvestris* L.) and Norway Spruce (*Picea abies* (L.) Karst.) (Berglund et al., 2013). In that study, sawing simulations of logs in their optimal rotational position with regard to knot structure and outer shape were carried through. A value increase of 13 % was obtained when knot information was accounted for compared to sawing logs in a traditional way.

Detailed knot data is also valuable at the log sorting station, where logs are measured and sorted into different piles depending on size, shape and quality. Studies have shown that discrete x-ray scanning can be used to sort logs based on interior quality and this manner of sorting can be used to improve the quality of the sawn timber (Oja et al., 2004, 2005). It is reasonable to expect that by using more detailed knot data from a CT scanner, quality sorting can be more accurate.

If a log is CT scanned moments prior sawing, then a decision of how it should be sawed must be done in seconds. Degrees of freedom at log breakdown, such as log spatial position, log rotational position and sawing pattern used, make this optimization task difficult. If all possible choices of sawing parameters would be simulated in a brute force manner, the necessary computational time would be large. Therefore, it would be beneficial to develop alternative algorithms to lessen the computational burden.

The purpose of the work with this licentiate thesis is to develop means to extract knot information automatically from images obtained from a high speed industrial CT scanner. Additionally, this thesis should evaluate how information of knots from such a scanner could be used successfully in the industry.

The objectives and delimitations of the research are to:

- Develop a knot detection algorithm for Scots pine (*Pinus sylvestris* L.) and Norway spruce (*Picea abies* (L.) Karst.). The algorithm should be robust with a high detection rate and a low amount of falsely detected knots. Knot position, size, length and dead knot border, i.e. the position where knots transitions from sound to dead will be extracted.

- Develop a method to decrease the computational time when optimizing log rotational position by projecting all knots to a plane. Validate

the performance of the algorithm on Scots pine and Norway spruce.

- Investigate the impact on value recovery for a sawmill using a high speed industrial CT scanner at the saw line if the sawmill sells strength graded centre boards of Norway spruce. The value recovery is compared to sawing all logs in horns down position.

Chapter 2

Background

2.1 Principles of the sawmill process

Figure 2.1 shows the main steps in the sawmill industry process that starts with trees in the forest and ends with products sold to customers. Forestry machines cut down trees into several logs typically of about four meters in length. The logs are transported to a sawmill and sorted with respect to mainly diameter and in some cases other features as well. Logs are then debarked and sawed into boards of varying dimensions. The boards are then sorted in the green sorting station before they are dried to a specified moisture content. After drying, the boards are trimmed to specific length modules, sorted to different grades and are either sold or subjugated to further processing. Examples of such processing are plaining, gluelam beam production and construction of housing products. Although the process may differ between sawmills, the process described in this section is typical for a Scandinavian sawmill processing Norway spruce (*Picea abies* (L.) Karst.) and Scots pine (*Pinus sylvestris* L.).

2.1.1 Log sorting station

When logs first arrive to a sawmill they are put through the log sorting station. This part of a sawmill has mainly two purposes; determining the price of the logs to be paid to the forest owners and sorting the logs into

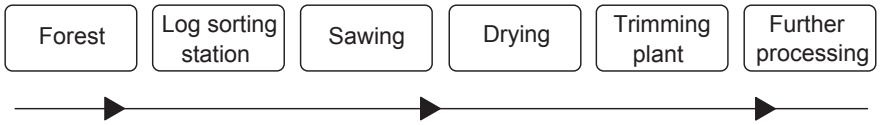

Figure 2.1: The typical main steps for the raw material flow of the sawmill industry.

sorting classes to better control the breakdown process. Which sorting class a log is put into is determined by various log properties such as top diameter, crook, taper and, if the information is available, internal quality measurements. The measurements are done automatically with scanning equipment, which may be optical (i.e. laser based) or x-ray based. Sorting classes are chosen so that logs that are suitable to be sawed with the same settings of the sawing line are grouped together. In practice, logs with similar diameter are put into the same sawing class.

2.1.2 Sawing line

When sawing, a batch of logs are picked from the same sorting class and transported to the saw intake, where each log is fed sequentially. All logs are then debarked (which for some sawmills are done when logs first arrive at the sawmill) and then the logs are scanned by a measurement system to obtain the orientation of the logs. This facilitates a rotation of the logs to a specific position. Usually this is horns down or at the position that will optimize the volume yield in the breakdown process. Horns down is defined as the rotational position so that the crook of the log is directed upward as shown in Figure 2.2.

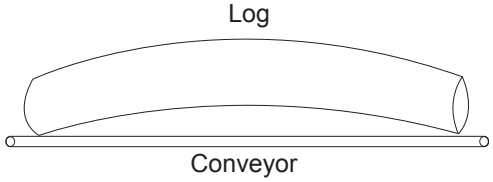

Figure 2.2: Definition of horns down position. Both ends of the log rests on a conveyor belt while the crook is directed upward.

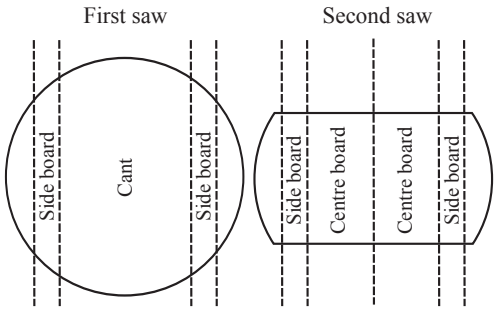

Figure 2.3: Square sawing. The first sawing machine cuts the log into side boards and a cant. The cant is then rotated by 90 degrees and cut by the second sawing machine into side boards and centre boards. Side boards are further processed by edging and trimming, while trimming is the only operation on centre boards (Berglund et al., 2013).

Although there are many ways to saw a log, this thesis investigates the most common in Scandinavian sawmills, namely square sawing. A description of square sawing can be seen in Figure 2.3. Modern second saws (see Figure 2.3) are able to curve saw, i.e. follow the curvature of the log, to get a higher yield. All side boards are subjugated to edging, which means cutting the boards to the correct width.

A core setting of the saw line is the sawing pattern, which determines the width and thickness of each outgoing board. Also the number of boards taken from each log is determined by the sawing pattern. The sawing pattern can be thought of as the position of the dashed lines (cuts) in Figure 2.3. It is crucial to choose appropriate sawing patterns to each sawing class to optimize the sawing process.

The volume yield when sawing logs can be defined in various ways. In this thesis, the definition is the volume of dried, edged and trimmed sawn timber divided by the total volume of the logs. Depending on log diameter and sawing pattern, the volume yield varies, but a rule of thumb is that it rarely exceeds 50 % for any log.

2.1.3 Trimming plant

After log breakdown, the boards are sorted by dimension and dried in kilns which causes boards to deform and shrink. The next step in the

process is the trimming plant where boards are trimmed to specific length modules, then graded and sorted with respect to grade. The sorting is either done automatically or manually according to a standard that describes the requirements put on boards. There are several standards for different purposes and in this thesis, two standards used in Scandinavia are included: Nordic timber grading rules (Anon, 1997), which is grading with respect to appearance, and INSTA142 (SS 230120) that is a visual strength grading standard. The former standard measures visible features with purpose of determining the visual appearance. The latter specifies requirements for visual features, such as annual ring width, deformations, splits, and knots, with purpose to determine the strength of the boards.

2.2 Defects in logs

Features and defects in trees varies with species and growth conditions. The value of wood products of Scandinavian Norway spruce and Scots pine depends on features and defects such as annual ring width, heartwood content, rot, splits, resin pockets, spiral grain, compression wood, knots, and top ruptures. This thesis focuses on a few of these, which are explained in more detail. The properties described in this section specifically refer to Norway spruce and Scots pine unless stated otherwise.

2.2.1 Density and heartwood

Density of wood consists of mainly two parts; wood fibre and moisture (water). Norway spruce and Scots pine develop something called heartwood. It contains less water than sapwood and occurs at the radial center of the tree. Butt logs (logs from the lowest part of trees) have a larger amount of heartwood than top logs, which in some cases do not have any heartwood at all. Figure 2.4 shows x-ray images of a cross-section of both a pine and a spruce log taken with a CT scanner. The dark areas in the center of the logs are heartwood. Wood outside of the heartwood is called sapwood.

(a) Norway spruce (b) Scots pine

Figure 2.4: CT slice of a Norway spruce and a Scots pine log.

2.2.2 Knots

Branches on Scots pine and Norway spruce trees are not only located outside the stem. They propagate all the way to the pith, which is the growth origin of the tree. Knots are the part of branches that are inside of stems and they cause severe fibre distortions. They have approximately the same density as sapwood and, therefore, the part of knots that are in the heartwood appears as high density objects. Knots can be either sound or dead and a knot is sound as long as it belongs to a living branch to the tree. When the tree no longer needs the branch, the tree will no longer sustain it. The branch gradually dies and parts of it will eventually become overgrown by the stem. Dead knots are partially dried out and are therefore of lower density than their sound counterparts. For Norway spruce and Scots pine, generally knots dies off at the bottom of the tree first.

On boards, knots are dark and the shape is different depending on at which angle the saw blade cut through the knots. Knots degrade boards and dead knots are often considered worse than sound ones (Anon, 1997). Although, for board strength, sound and dead knots are often considered equally degrading (SS 230120).

Figure 2.5: Board with a very steep splay knot. Most likely due to a top rupture.

2.2.3 Top rupture

A top rupture occurs when the top of a tree gets damaged in its youth. The most common reasons of this in Scandinavia are moose feeding on the top of the tree and heavy snow load. When this occurs, the tree survives by letting one of the existing branches become the new top which results in a severe crook. This crook will eventually be overgrown and smoothed out when the stem expands and can in general not be seen on the outside of a full grown tree. The old top will become a knot with a very steep incline, which might lead to ugly visual appearance of boards as shown in 2.5. Knots of this type also reduce board strength severely.

2.3 Properties of boards

2.3.1 Wane

Wane on boards appears when the sawing pattern lies partially outside any cross section of a log. Then the outer shape of the log gets included on the edges of the board. This occurs usually at the top end, where the log diameter generally is smaller. Wane both affect visual appearance and strength of boards, which might cause a degrading of boards depending on the sorting rules and the severity of the wane present.

2.3.2 Strength

When using timber in load-bearing constructions, knowledge of the strength and stiffness of each component is crucial. Bending strength of boards, or simply board strength, are measured in MPa and defined as the maximum stress applied to a board before breaking. Exact measurements require destructive testing and this can obviously not be applied on boards aimed for

any practical use. There are currently two types of measurements in use to approximate board strength without breaking the boards, namely machine strength grading and visual strength grading. In machine strength grading, boards are passed through a machine that measures one or several parameters including the modulus of elasticity to approximate the stiffness and strength of the boards. Visual strength grading predicts board strength by ensuring that visual features of the boards are within certain criteria determined by a grading rule.

Visual features of boards that affect the strength are size of knots, placement of knots, knot groupings, wane, top ruptures, annual ring width, deformations, splits and spiral grain. Features based on knots are the most important ones together with wane.

2.3.3 Board grading

Section 2.1.3 describes two board sorting standards: Nordic timber grading rules and INSTA142. The Nordic timber grading rules have grading classes A, B, C and D, where A is divided into the subclasses A1, A2, A3 and A4. A is the highest grade while D is the lowest. The classes for INSTA142 are T3, T2, T1 and T0, which correspond to bending strengths of 30, 24, 18 and 14 MPa respectively.

2.4 Measuring wood with x-rays

The benefit of using x-rays when scanning wood instead of light in the visual spectra (i.e. laser) is that x-rays penetrate the material. x-ray absorption of a material depends on the density as well as the distance the rays have travelled through the material. Measurements of the remaining x-ray intensity level after the rays have travelled through a piece of wood can therefore estimate the density of the material.

2.4.1 Discrete x-ray scanning

There are modern measurement equipment for both boards and sawlogs where x-ray scanning is included. For sawlogs, such equipment usually include one or two fixed x-ray planes that penetrate the sawlogs as they move

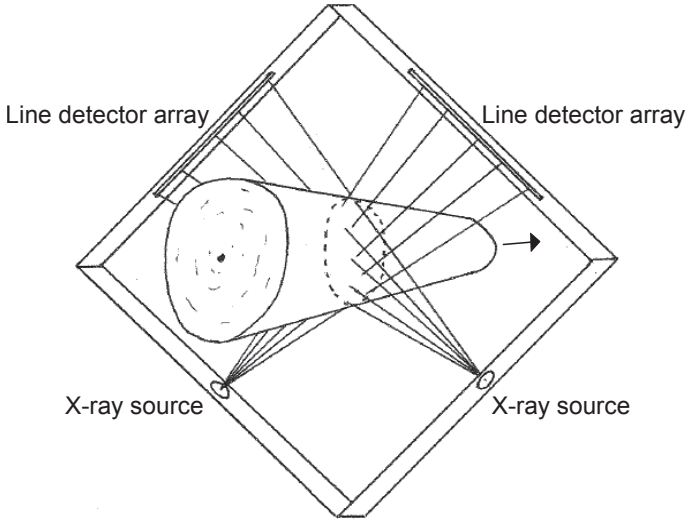

Figure 2.6: A schematic picture of discrete scanning with two x-ray sources is shown in this image. Logs travels on a conveyor in lengthwise direction. At any given moment, the x-ray planes produce one dimensional density profiles of a slice of a log. When combining density profiles of all log slices, a two dimensional density image of the log for each x-ray source will be generated.

on a conveyor belt. Figure 2.6 shows a system using two x-ray sources. The resulting x-ray images contain information enough to estimate heartwood content, dry density, knot whorl position and knot volume. However, rot, pitch pockets, checks and exact position of knots cannot be seen. Therefore, the process of the sawmill cannot be optimized with respect to these features.

2.4.2 Computed tomography

Sawlogs can be scanned using computed tomography (CT). A wide range of properties and features can be seen in detail, such as knot structure, pith, heartwood content, density, pitch pockets, bark, top ruptures and checks. The obtained level of detail depends on the resolution and error levels of the scanner.

For scientific research, CT scanning of sawlogs has been done for decades, but the scanners used have been too slow for industrial appli-

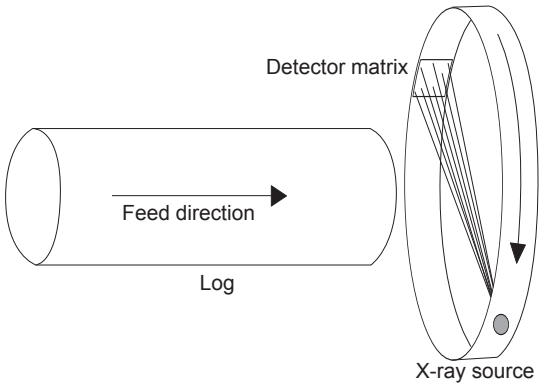

Figure 2.7: High speed CT scanning of sawlogs using a cone beam x-ray source.

cations with slow reconstruction algorithms as a bottleneck. However, Katsevich (2004) describes a faster reconstruction algorithm which is now implemented in a high speed industrial CT scanner (Giudiceandrea et al., 2011). With that scanner, it is possible to scan sawlogs at production speed.

That scanner uses an x-ray source emitting a cone beam of radiation passing through the objects scanned. The detectors are organized in a two dimensional array. Both the x-ray source and the detector array rotates while logs passes through making it a spiral scanning. With this specific equipment, logs can be transported in over two meters per second. Figure 2.7 shows a sketch of the equipment.

The exact benefits of using such a scanner are not fully evaluated and one purpose of this thesis is to investigate this. There are currently three scanners of this type in use and the strategies used by these sawmills are different. One sawmill CT scans logs of expensive species and manually analyze the images to optimize the breakdown for each individual log. The production speed in this case is low because of the costly raw material. Another company uses a scanner to locate the knot free zone in pruned Radiata pine (*Pinus radiata* Don) logs. By doing this, veneer production can be optimized. The third company is a sawmill that uses a scanner on whole stems to, for instance, find optimal bucking positions. Other possible applications are log rotation optimization when sawing and log quality sorting at the log sorting station.

Chapter 3

Method

3.1 The pine and spruce stem banks

The material used in the papers of this thesis is logs that come from the pine stem bank (PSB) (Grönlund et al., 1995) and the European spruce stem bank (ESSB) (Berggren et al., 2000). The PSB consists of about 600 Scots pine (*Pinus sylvestris* L.) logs from different plots in Sweden while the ESSB includes about 800 Norway spruce (*Picea abies* (L.) Karst.) logs from Sweden, Finland and France. In both data banks, stems in different diameter classes were chosen and the logs were scanned with a medical CT scanner (Siemens SOMATOM AR.T). The resulting CT images show the log outer shape, as well as internal features such as pith location, sapwood-heartwood border and knots. The knots are described by nine parameters specifying size and position in the log as well as if knots are fresh or dead (Oja, 2000).

3.2 Datasets

In the papers of this thesis, subsets of the PSB and the ESSB were chosen. Number of logs, species and denotation of the datasets are described in Table 3.1.

Dataset A consists of 10 pine and 8 spruce logs chosen so that a wide range of defects and properties are included. Except from top diameter,

Table 3.1: Datasets used in the publications.

Name of dataset	Number of logs	Species (pine/spruce)	Publication used in
A	18	Both	I
B	47	Pine	I
C	95	Pine	II
D	677	Spruce	III

the properties important in the selection were heartwood content, heartwood shape, rot content, top ruptures, density, knot structure and knot size. The purpose of this dataset was to evaluate the precision of the algorithm presented in Section 3.3 when measuring knot position, size and length.

In a previous study (Grönlund, 1995), pine logs from the PSB were sawn to boards and the dead knot border was measured on the planks. Dataset B consists of 47 pine logs from that study. The purpose of this dataset was to measure the precision of dead knot border measurements of the knot detection algorithm.

Dataset C consists of the logs in the PSB that have a bow height of less than 14 mm and a difference between sawing pattern diagonal and top diameter of more than 18 mm. The concept of sawing pattern diagonal is explained in Figure 3.1. Dataset C is used in Paper II and logs were excluded from the PSB in this way to avoid wane when calculating the optimum rotational position of the logs as explained in Section 3.4.2.

Dataset D consists of all logs in the ESSB that have a top diameter between 130 mm and 384 mm. Logs outside this range are excluded because logs outside that interval were not considered interesting for the production strategies evaluated in Paper III, where the dataset was used.

3.3 Detecting knots in CT images

Detection of knots in CT images is difficult because no two knots are identical. In fact, knots from the same species of wood can look very different in CT images as shown in Figure 3.2. A computerized algorithm

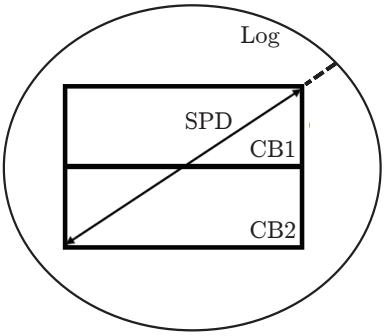

Figure 3.1: A log seen from the top end, where SPD means sawing pattern diagonal and CB means center board.

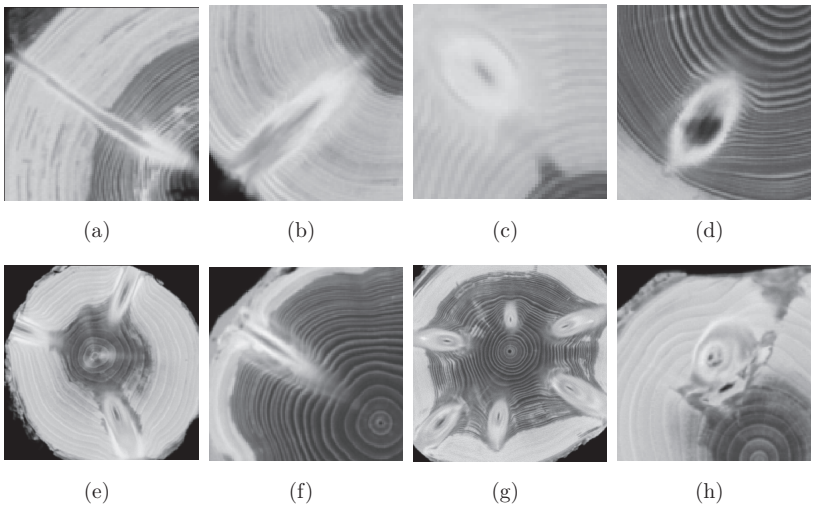

Figure 3.2: Examples of knot appearance in CT images. Figure (a)-(d) are from Scots pine logs and (e)-(h) are from Norway spruce logs.

needs to account for logs with different properties and features to avoid falsely detected knots.

Paper I describes an algorithm to detect knots in Scots pine and Norway spruce. Figure 3.3 shows the main steps in the proposed algorithm and explanations of each step follow below. A more detailed description is presented in Paper I.

3.3.1 Indata

Aside from CT images of the log, the knot detection algorithm requires three inputs: The borderline between bark and clear wood, the borderline between sapwood and heartwood and the pith position in the images. These three inputs are shown in Figure 3.4. Bark-wood border is required since there is no need to detect knots in the bark. The proposed algorithm uses the fact that the wood density of heartwood and sapwood differs. Segmentation of knots is done differently in heartwood compared to sapwood and therefore, the information of which areas that are heartwood and sapwood respectively is vital for the algorithm. Knots originate from the pith and to create accurate models of knots, the position of the pith must be known.

3.3.2 Creating concentric surfaces

The first step in the algorithm is to create concentric surfaces. A concentric surface is similar to a cylindrical shell, but with a major difference in how the radius is defined. Slightly simplified, the radius is defined so that the concentric surfaces approximately follow the annual rings of the log, instead of having a circular shape.

A total of ten concentric surfaces are created, where at least five are in the heartwood and the rest in the sapwood. With increased heartwood content in logs, the portion of concentric surfaces that are placed in the heartwood is increased. Knot detection in heartwood is easier than in

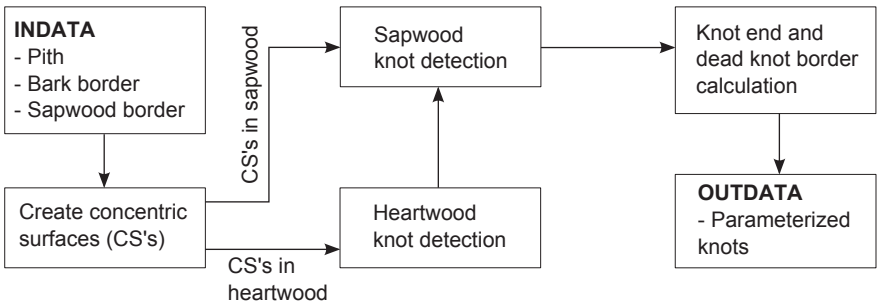

Figure 3.3: Flow chart of the main steps in the knot detection algorithm.

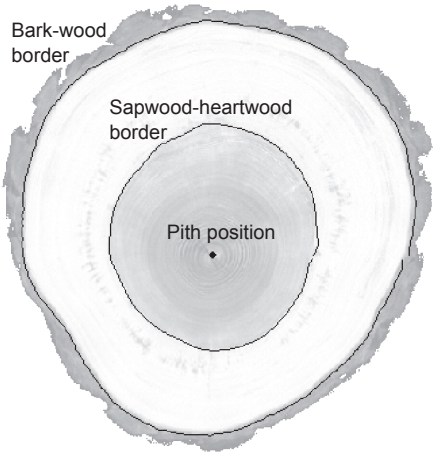

Figure 3.4: The three types of input data required by the knot detection algorithm. X-ray intensity values are intentionally brightened.

sapwood, that is the reason for creating at least five concentric surfaces in the heartwood. A concentric surface in the heartwood is showed in Figure 3.5.

3.3.3 Knot segmentation in heartwood

In the next step, high density objects are segmented from the concentric surfaces in the heartwood. This is done by first filter the concentric surfaces with a rectangular median filter to obtain the background, where the

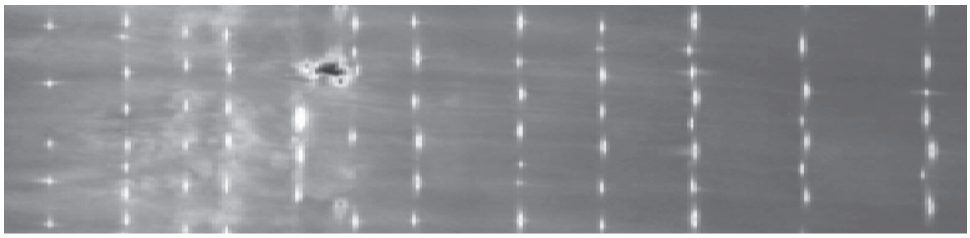

Figure 3.5: Example of a concentric surface in the heartwood.

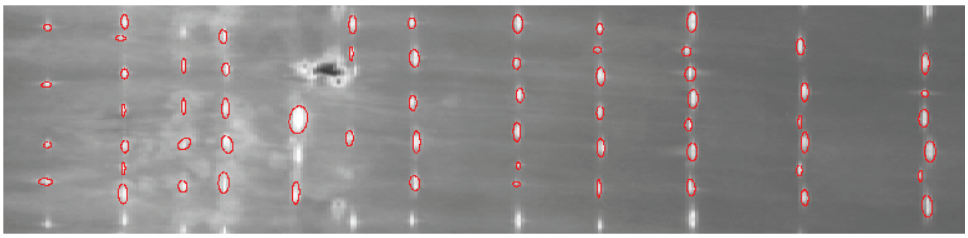

Figure 3.6: Knots detected in the heartwood showed in one concentric surface. Ellipses that could not be matched to other ellipses in between concentric surfaces have been deleted.

Table 3.2: Knot parameterization models. $A, B, \ldots, I$ are the parameters that are unique for each knot. All parameter models are first presented in Grönlund et al. (1995) except lengthwise position, which is described by Andreu and Rinnhofer (2003).

Knot feature	Parameter model
Knot diameter (rad)	$\phi(r) = A + Br^{1/4}$
Lengthwise position (mm)	$z(r) = C + D\sqrt{r} + Er$
Angular position (rad)	$\omega(r) = F + G\ln(r)$
Knot end (mm)	H
Dead knot border (mm)	I

foreground consists of knots and other relatively small objects. Using the background image as variable threshold values, objects in the foreground are segmented. Simple put, objects that have a relatively high density compared to the background are segmented in this way. All segmented objects in the resulting binary image are fitted to ellipses. Ellipses with unrealistic shape or size are unlikely to be knots and are therefore deleted.

Overlapping ellipses from consecutive concentric surfaces are matched together. Ellipses that do not have any counterparts in other concentric surfaces are deleted to get rid of false positives. Figure 3.6 shows the resulting knots in one of the concentric surfaces.

Size and position of each knot are then parameterized using the regression models in Table 3.2. Figure 3.7 shows how the different knot geometries are defined.

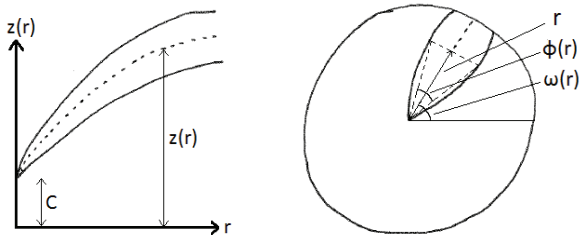

(a) Knot lengthwise position.

(b) Knot angular position and size.

Figure 3.7: (a) is showing how lengthwise position, $z(r)$, of the knot axis (dotted line) is defined as a function of the distance from pith, r. $z(r)$ is measured in the log's coordinate system. The constant, C, is the distance from the bottom of the log to the start of the knot. In (b), the definitions of knot angular position, $\omega(r)$, and knot diameter, $\phi(r)$, are described. Both are angles that varies for different values of r.

3.3.4 Knot segmentation in sapwood

Segmentation of knots in sapwood is hard since knots may appear differently depending on individual logs, and sometimes individual knots. In some cases, knots are of slightly higher density than surrounding wood, while other times, knots are less dense. Often, knots have the same density as the surrounding wood, but with a different texture. Examples of knot appearance in sapwood can be seen in Figure 3.8.

The proposed algorithm approaches this task by extrapolating each knot that was found in the heartwood to the first concentric surface in the sapwood. A subimage of the concentric surface is extracted around each knot and a series of steps are performed on the subimages to determine the position and size of the knot. First, the standard deviation of each row and column of the subimages are calculated to determine whether there exists an object in the subimage or if the knot has ended before reaching this concentric surface. To determine the size and position of the object, a morphological dilation method is applied. This method is successful on a subset of all knots. For other knots, an ellipse is created in the subimage from the knot parameterization data.

When knots in the first concentric surface in the sapwood are detected, the knot parameters are updated with the regression models. The knots are then extrapolated to the next concentric surface and so forth.

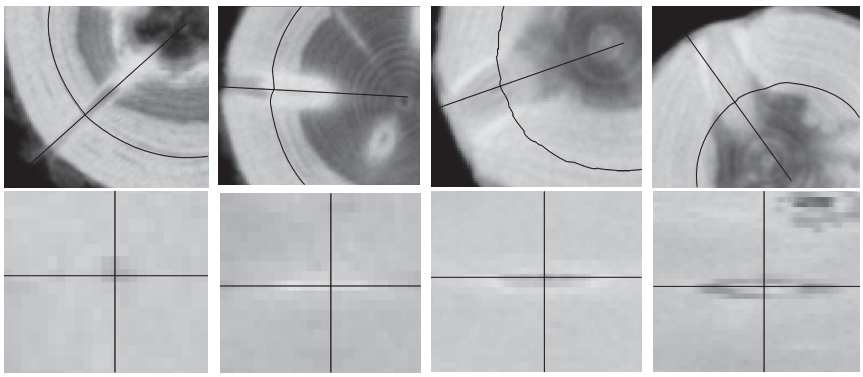

Figure 3.8: Examples of Scots pine ((a)-(b)) and Norway spruce ((c)-(d)) knots in sapwood. The upper images are CT slices and the lower are subimages of concentric surfaces at the intersection of the lines in the upper images.

3.3.5 Knot end and dead knot border

Knot end is set to the midpoint between the outermost concentric surface where the knot was located and the next concentric surface. If the knot was detected in the concentric surface closest to the log outer border, then knot end is set to the intersection of the bark-wood border and the knot axis.

Dead knot border is set for all knots to where each knot has the largest size. This position can be derived directly from the derivative of the knot size parameterization model. To improve dead knot measurements, outlying values are corrected in the way described in step 11 of the algorithm description in Paper I.

3.3.6 Outdata

The output from the algorithm is all detected knots in form of parameters to the regression models described in Table 3.2.

3.3.7 Determining precision of knot detection

The knot detection algorithm's precision of measuring knot size, position and length (end point) were evaluated on dataset A. To carry though this validation, ellipses were drawn manually in the concentric surfaces of the CT images to mark the knot position and size. These manual reference measurements were compared to the automatic measurements done by the algorithm. A detailed description of this is located in Paper I. Using dataset A, the hit rate and the amount of false positives were calculated. The precision of dead knot border measurements could be directly evaluated using the data provided in dataset B.

3.4 Production strategies

CT imaging opens up possibilities for sawmills to use new production strategies. Such strategies need to be investigated to see how they affect the profitability of sawmills. Some strategies are described in Section 2.4.2 and another is described in Berglund et al. (2013).

Both Paper II and III present case studies with purpose to show the profitability or loss for a sawmill to use the proposed strategy compared to a strategy that is industrial praxis today. These strategies are described in Section 3.4.2 and 3.4.3.

3.4.1 Sawing simulations

To calculate the outcome of log breakdown, computer assisted sawing simulation is convenient since each log can be sawed an infinite number of times. Comparisons of results using a different set of sawing parameters can therefore be evaluated. It is also much cheaper to saw virtual logs in a simulator software than to saw real logs for scientific purposes. For these reasons, evaluations of different sawing strategies has been done with sawing simulation.

The simulation software used is Saw2003, which is described in Nordmark (2005). Log outer shape and knot information can be accounted for with this software. Therefore, logs from the PSB and ESSB can be simulated. Optimization of trimming and edging of side boards and trimming

Table 3.3: Pricing of the qualities of sawn timber used in the simulations in Paper II. The prices are relative to each other.

Quality	A	B	C
Centreboards	1850	1600	1000
Sideboards	3000	1400	1100

Table 3.4: Price list with price differentiation between board grades for Paper III. The prices are relative with the price for centre boards of grade T2 as reference.

Board type	Centre boards			Side boards			Chips
Grade	T3	T2	Reject	A	B	C	-
Price/m^3	106	100	68	100	100	68	18

of centre boards with respect to value according to the grading rules described in Anon (1997) are built-in. Price per cubic meter for all quality grades must be provided. Paper II is using this software as it is, while Paper III uses an external trimming software in addition to SAW2003. That external software optimizes trimming of boards with respect to the strength grading system described in SS 230120.

For the knot projection algorithm in Paper II, all sawn timber are appearance graded according to the Nordic timber grading rules and the prices per cubic meter are shown in Table 3.3. The grades used are A, B and C grade. For Paper III, side boards are graded in the same way, but center boards are strength graded according to SS 230120 to T3, T2 and reject grade. The prices in this case are shown in Table 3.4. These studies investigate relative price differences. The absolute values in Table 3.3 and 3.4 are therefore irrelevant.

3.4.2 Knot projection algorithm

CT images from a log can in theory be used to optimize sawing parameters such as rotational position, spatial position, skew and sawing pattern. If a CT scanner is to be placed at the saw line, this optimization must be done very fast. A brute force method of simulating every possible choice of sawing parameters would require immense computational resources and

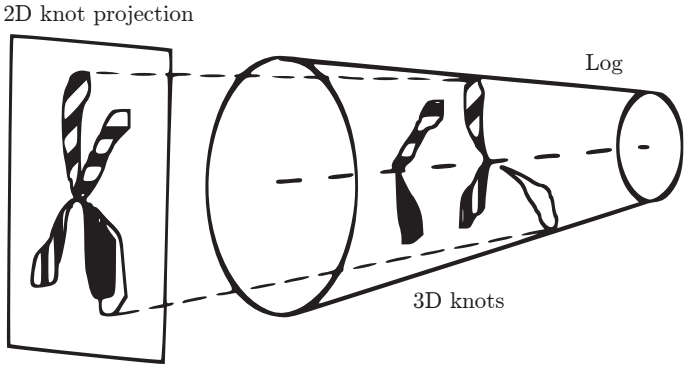

Figure 3.9: Projection of knots onto a plane perpendicular to the log lengthwise direction. Knots are patterned to illustrate which knot that belongs to each projection.

time. Therefore, it is important to investigate if any alternatives to the brute force method are feasible.

In Paper II, the proposed method is to project all knots from a three dimensional volume to a plane perpendicular to the log lengthwise direction according to Figure 3.9. A matrix with projected knots is made by summing the diameter values of all knots. Dead knots are scaled with the factor $\frac{10}{7}$ to address that such knots often are considered worse than sound knots (Anon, 1997). Knots with the smallest diameter are filtered out and the result is a matrix with weights corresponding to summed knot size. Center of gravity for the matrix is calculated and compared to saw pattern center position. Log rotational position for breakdown is chosen as the direction between these two points. This position is chosen with the purpose of letting the majority of the high impact knots be on the wide sides of the center boards (board face) instead of on the board edges.

Optimization of log rotational position according to the algorithm was evaluated on dataset C and compared to sawing logs in the horns down position. This evaluation was done with the sawing simulation software.

3.4.3 Full optimization for strength graded boards

The strategy that is investigated in Paper III is to use full information of knots and outer shape from CT images of logs to optimize the breakdown at a sawmill using square sawing. Breakdown of each log in dataset D

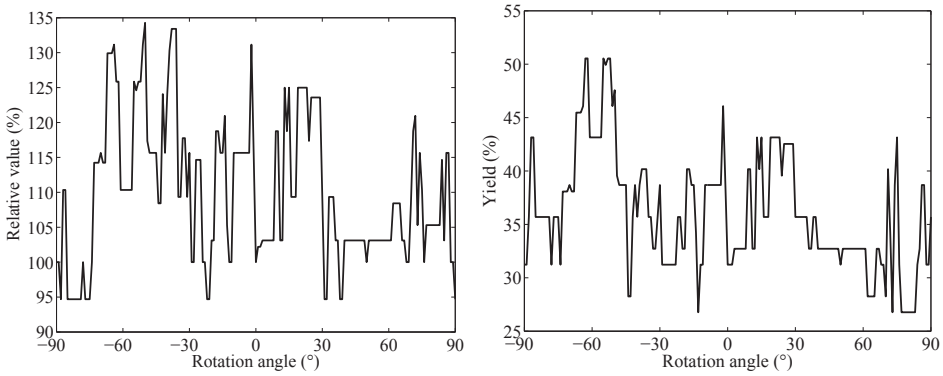

(a) Value (b) Yield

Figure 3.10: The value of all boards and chips (a) and yield (b) for $\theta \in [-90°, 90°]$. The value is relative to the value of 100 % at the horns down position where the rotation angle of $0°$ corresponds to the horns down position. The graphs represent one example log.

were simulated for rotational position $\theta \in [-90°, 90°]$, where $\theta = 0$ corresponds to horns down position. For each log, value and volume yield with respect to the θ-values form curves as in Figure 3.10. The maximum value for each log was compared to the corresponding value at horns down by calculating the ratio. Also the difference in yield between these two rotational positions were calculated.

3.4.4 Effects of errors in rotational position

In Paper II and III, errors in rotational position due to sawing machines have been considered. A rotational error in a sawing machine is assumed to be normally distributed $Z \in \mathcal{N}(\mu, \sigma)$), where μ is the expected value and σ is the standard deviation. Value of μ has been chosen to $\mu = 0°$ in both papers and σ was chosen to $\sigma = 6°$ and $\sigma = 5°$ in Paper II and III respectively.

Paper II evaluated this by adding the rotation error from the chosen distribution to both the horns down position and the proposed rotational position. The performance of the proposed algorithm with an error was evaluated versus the respective horns down position.

In Paper III, a Gaussian filter with $\sigma = 5°$ and window size $W_S =$

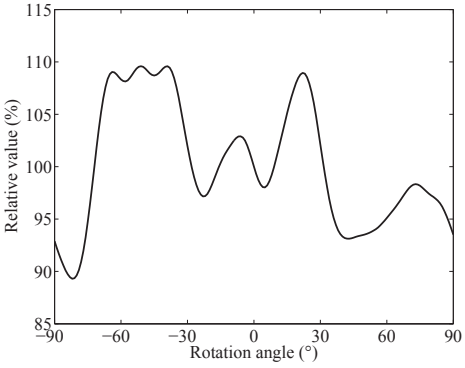

Figure 3.11: The filtered value function obtained by applying a Gaussian filter to the value function shown in Figure 3.10(a). The values are adjusted so that the value at horns down is 100 %.

$6\sigma - 1 = 6 \cdot 5 - 1 = 29°$ was applied to all value curves of the type in Figure 3.10(a). The new value functions appeared as in Figure 3.11 and the θ-value where those functions were maximized were chosen as the optimum rotational position. Thus, the strategy itself was changed with the knowledge of the rotation error.

3.4.5 Effects of errors in knot detection

Knot detection will never be completely precise. In Paper II, simulated errors in knot size, knot azimuthal direction and fresh knot length (distance from the pith to the dead knot border) was applied to evaluate the robustness of the knot projection algorithm. This evaluation was made using three different levels of normally distributed, non-systematical errors as described in Paper II. The size of the errors were chosen with help of experiences from Paper I.

Simulations and comparisons of board value and quality were carried out for the three error levels, using horns down sawing as well as rotating the logs according to the knot projection. In this case, the knots acquired from dataset C were considered to be the ground truth and were used as reference.

Chapter 4

Results and discussion

4.1 Precision of knot detection

Table 4.1 presents the number of reference knots manually measured, total number of knots found by the algorithm, percentage of reference knots found and percentage of falsely detected knots out of all knots detected by the algorithm. With only about 1 % of all found knots being false positives the algorithm is robust, which was the main objective. The algorithm found between 88 % and 94 % of all reference knots, which is a high number keeping in mind the low rate of false positives.

Table 4.2 shows the results from precision measurements of knot geometry, knot end and dead knot border. A positive mean error means that the algorithm overestimates the knot feature. The random errors in

Table 4.1: Number of reference knots manually measured, total number of knots found by the algorithm, percentage of reference knots found and percentage of falsely detected knots out of all knots detected by the algorithm.

Species	Number of reference knots	Reference knots found	Total amount of found knots	Falsely detected knots
Pine	127	94 %	795	1.0 %
Spruce	119	88 %	1095	0.91 %

Table 4.2: Error measurements on knot diameter, knot position, knot end and dead knot border. Denotations for knot lengthwise position, knot angular position and dead knot border are z position, ω position and DK border, respectively. Validation of dead knot border for spruce was not included in this study and was intentionally left blank to clarify this.

Species	Knot feature	Mean error	SD of error
Pine	Diameter (mm)	-0.93	4.6
Pine	z position (mm)	-2.6	9.2
Pine	ω position (°)	0.34	2.3
Pine	Knot end (mm)	-14	21
Pine	DK border (mm)	-4.0	12
Spruce	Diameter (mm)	0.93	5.1
Spruce	z position (mm)	-0.93	7.8
Spruce	ω position (°)	-0.19	1.9
Spruce	Knot end (mm)	-16	29
Spruce	DK border (mm)	-	-

measuring z-position were 9.2 mm and 7.8 mm for pine and spruce, respectively. These values are low since they are less than the z-resolution of the CT images, which is 10 mm. In the case of angular position, the achieved random errors of about 2° is low compared to a typical rotation positioning error in a saw-line of $5° - 6°$.

Automatic measurements of knot end have relatively high errors. The problem is underestimation, which is due to insufficient knot detection in sapwood. The algorithm has a tendency to lose track of knots in the sapwood because of small contrast between knots and surrounding wood.

A study on Scots pine (*Pinus sylvestris* L.) by Grundberg (1999) presents how various error levels on knot diameter and dead knot border affect estimated product value. According to that study, a random error of 10 mm in dead knot border and 6 mm in maximum knot diameter (which is roughly what was achieved in this article) generate a product value 6.5 % lower than the reference value with no errors. If the error in diameter is decreased to 3 mm, the value difference becomes 1.7 %. When doing the opposite; keeping diameter error at 6 mm and decreasing dead knot border error to 5 mm, the value difference becomes 6.3 %. Improved

diameter measurements would therefore benefit the algorithm more than improved dead knot border calculations.

4.2 Simulation technique – Knot projection

For the 95 logs tested in Paper II, the average value change from sawing horns down compared to sawing based on the proposed knot projection method, was 2.2 % in favor for the knot projection method. This is low compared to 14-16 % that was achieved by Berglund et al. (2013) and also compared to what was achieved in Paper III, which was 11 %.

The value potential distribution for the 30 runs when sawing in a random rotational position had a 95 % confidence interval, for the mean, of (1.43 %, 1.97 %). Since it was 30 independent, random test runs, the central limit theorem states that the distribution will be approximately normally distributed. This confidence interval can be compared to sawing the logs according to the knot projection, which resulted in a mean value increase of 2.2 %, which is thus above the confidence interval of the random rotation value distribution.

When a rotational error was added to the sawing simulation of the 95 logs, the average value change was +1.3 % when sawing based on the knots, compared to horns down. The corresponding value change when relatively small errors in knot position and size were added, was +1.9 %. The error levels were small compared to what was presented in Paper I.

There is no perfect knot detection algorithm or positioning equipment at the saw line. The proposed algorithm will not be suitable for industrial use in its present shape since it will not be better than pure chance. Even in ideal conditions, the method is just slightly better than chance and do not reach the performance of brute force methods.

One should bear in mind that the method was tested on a selection of logs in the PSB, which corresponds to about $\frac{1}{6}$ of the entire population of logs. The reason for doing this was to reduce the effect of the outer shape of the log, since this is not accounted for in the projection method. The implication of this choice is however that the results presented here are only representative for a sample of selected logs.

One of the main advantages of the proposed method is that it assesses a projection of the information available in CT data, thus decreasing com-

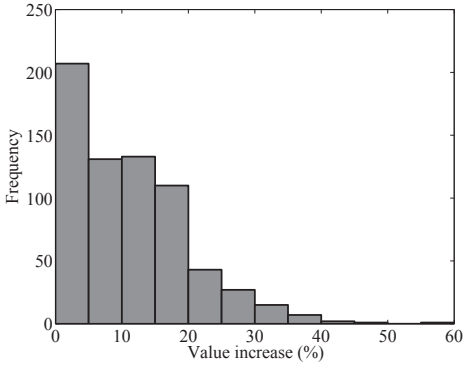

Figure 4.1: Value increase in percent compared to the horns down position if using the log rotation that maximizes the total value of the strength graded centre boards, appearance graded side boards and chips. Frequency on the y-axis represents number of logs.

putational time compared to a full optimization. This is important in an industrial situation, were a breakdown decision needs to be made for each individual log, in a short time frame. The saved computational time could be used for assessing translational position of the log, sawing patterns or other decisions related to the breakdown procedure.

4.3 Production strategy – Strength graded boards

The average value increase in Paper III when considering the total value of centre boards, side boards and chips are 11 % for an ideal rotation. With a rotational error applied, the corresponding value increase is 6 %. Change in volume yield is 2 % in average for an ideal rotation and 1 % in average with a rotational error present. A histogram of value increase is presented in Figure 4.1. From the simulations, it is evident that a rotational error to the sawing machine reduces the average value increase, but that it is still profitable to rotate each log individually to obtain a higher value recovery. This means that a reduction in rotational error of the saw line results in a higher value recovery for a sawmill with a production strategy similar to the case in this study.

If only the value of the center boards is considered instead of including

all products, the mean value increase compared to the horns down position is 11 %. With a rotational error, the mean value increase drops to 6 %. The corresponding change in volume yield is 0 % in average both for an ideal rotation and with a rotational error. The value changes are identical to the case when all products were considered.

Adding in that Berglund et al. (2013) achieved 14 % mean value increase when sorting spruce logs according to the Nordic timber grading rules (Anon, 1997), it can be concluded that the method of rotating logs to an optimal position prior sawing is robust with respect to which grading rules that are used. Optimizing with respect to the Nordic timber grading rules on all products, INSTA142 (SS 230120) on centre boards or a hybrid between the two standards, all give a mean value increase of 11-14 %. When a rotational error is present, each value increase drops to 6 %.

Chapter 5

Conclusions

- Paper I – Knot detection algorithm
  - Paper I presents the first published and validated knot detection algorithm on high speed computed tomography images. It is a good benchmark when evaluating other knot detection algorithms.
  - The proposed knot detection algorithm had a high knot detection rate and had low amounts of false positives when validated on logs with large variety in properties.
  - Future work should prioritize better diameter measurements in heartwood and better knot detection in sapwood to improve precision in knot diameter and knot end measurements.
- Paper II – Knot projection as simulation technique
  - The proposed knot projection algorithm is most likely faster than brute force simulation techniques.
  - Rotational errors and small errors in knot detection make the proposed projection algorithm equally good as pure chance, thus making it unsuitable for practical use in its current state. Knot projection as a concept can although not be dismissed completely.

- Paper III – Rotating logs to optimize value of strength graded boards
  - The production strategy to rotate logs to optimize the value of the sawn timber showed a mean value increase of 11 %. The corresponding value when a rotation error is present was 6 %.
  - The value increase when rotating logs are robust with respect to which grading rules that are used. This is true both in the ideal case and when a rotational error is added.

Chapter 6

Future work

6.1 Knot segmentation

It can be concluded that, for knot detection, future work should prioritize improvements in knot size measurements. Species should be kept separate in future work due to differences in knot appearance between species. Dead knot border is closely related to maximum knot diameter (Grönlund, 1995) and improvements in knot diameter measurements would increase the accuracy of detecting dead knot border. Detection of knots in sapwood needs improvement to get more accurate knot end measurements. This is likely the hardest part when detecting knots.

6.2 Sawing simulation techniques

In the case of optimizing log breakdown with knot projection, future work includes adding other defect types such as rot or pitch pockets to the data. These could be projected and weighted in the same manner as the knots, and in the case of these defects it is also desirable to turn the log so they end up on one half of the sawing pattern. The direction in which to rotate the logs could be more distinct in that case, but it is not certain. The effect of outer shape of the log should also be included. Some projection method might be used to sort out the worst rotational positions to decrease the computational time.

6.3 Production strategies

When optimizing the value when centre boards are strength graded, an interesting study would be to include density and additional kinds of defects. These include top ruptures, annual ring width, splits and spiral grain. That would give a more accurate visual strength grading. Another interesting study would be to increase the degrees of freedom in the sawing simulation. Inclusion of optional skew and spatial position of logs in addition to rotational position would increase the optimization potential although the computational burden would increase as well. If some of the defects would be projected as described in Paper II, the time for computation would be lower.

Although Paper II and III in this thesis focus on having a CT scanner at the saw line, it would be interesting in future studies to evaluate the profit of placing such equipment at the log sorting station. The major advantage of that is the possibility to sort logs into sawing classes based on specific internal features. For example, logs with low pitch pocket content could be sorted out and used for timber addressed to furniture production, where pitch pockets visible on board surfaces are very expensive to deal with.

A thrilling though is to use a CT scanner at the log sorting station and store the information of all logs when they first arrive at the sawmill. Then there would be plenty of time to calculate optimum sawing parameters since logs likely lie sorted into piles on the log yard for hours or days prior sawing. When a specific log arrives at the sawing line, the sawing machines could download information of optimal parameters specifically for the current log. This system requires that a log scanned with the equipment available at the saw line can be matched to the CT images of the same log acquired at a previous time. There might be thousands of logs to choose from when performing the matching and it is a challenge to make such a matching robust and fast.

References

Andreu, J.-P. and A. Rinnhofer, 2003: Modeling of internal defects in logs for value optimization based on industrial CT scanning. *Fifth International Conference on Image Processing and Scanning of Wood*, A. Rinnhofer, Ed., Bad Waltersdorf, Austria, 141–150.

Anon, 1997: *Nordic Timber: Grading rules for pine (Pinus sylvestris) and spruce (Picea Abies) sawn timber: Commercial grading based on evaluation of the four sides of sawn timber.* Föreningen svenska sågverksmän (FSS), Sweden.

Berggren, G., S. Grundberg, A. Grönlund, and J. Oja, 2000: Improved spruce timber utilisation (STUD). Tech. rep., Luleå University of Technology and AB Trätek. European shared cost research project within FAIR (DGXII/E2), contract no. FAIR-CT96-1915. Final report sub-task A 1.2. Database and non-destructive "Glass-log" measurements.

Berglund, A., O. Broman, A. Grönlund, and M. Fredriksson, 2013: Improved log rotation using information from a computed tomography scanner. *Computers and Electronics in Agriculture*, **90**, 152–158, doi: 10.1016/j.compag.2012.09.012.

Giudiceandrea, F., E. Ursella, and E. Vicario, 2011: A high speed CT scanner for the sawmill industry. *17th International nondestructive testing and evaluation of wood symposium*, F. Divos, Ed., Sopron, Hungary.

Grönlund, A., L. Björklund, S. Grundberg, and G. Berggren, 1995: Manual för furustambank. Tech. Rep. 19, Luleå tekniska universitet, Luleå. In Swedish.

Grönlund, U., 1995: Quality Improvements in Forest Products Industry. Ph.D. thesis, Luleå University of Technology.

Grundberg, S., 1999: An X-ray LogScanner – a tool for control of the sawmill process. Ph.D. thesis, Luleå University of Technology, Luleå, Sweden.

Grundberg, S. and A. Grönlund, 1998: Feature extraction with aid of an x-ray log scanner. *Proceedings from the 3rd International Seminar/Workshop on Scanning Technology and Image Processing on Wood*, O. Lindgren, A. Grönlund, and O. Hagman, Eds., Luleå University of Technology, Skellefteå, Sweden, 39–49, technical Report 1998:27.

Katsevich, A., 2004: An improved exact filtered backprojection algorithm for spiral computed tomography. *Advances in Applied Mathematics*, **32 (4)**, 681–697, doi:10.1016/S0196-8858(03)00099-X.

Nordmark, U., 2005: Value recovery and production control in the forestry-wood chain using simulation technique. Ph.D. thesis, Luleå University of Technology, Luleå, Sweden.

Oja, J., 2000: Evaluation of knot parameters measured automatically in CT-images of Norway spruce (*Picea abies* (L.) Karst.). *European Journal of Wood and Wood Products*, **58 (5)**, 375–379.

Oja, J., S. Grundberg, J. Fredriksson, and P. Berg, 2004: Automatic grading of saw logs: A comparison between X-ray scanning, optical three-dimensional scanning and combinations of both methods. *Scandinavian Journal of Forest Research*, **19 (1)**, 89–95, doi: 10.1080/02827580310019563.

Oja, J., S. Grundberg, and A. Grönlund, 2001: Predicting the stiffness of sawn products by x-ray scanning of norway spruce saw logs. *Scandinavian Journal of Forest Research*, **16 (1)**, 88–96, doi: 10.1080/028275801300004442.

Oja, J., B. Källsner, and S. Grundberg, 2005: Predicting the strength of sawn wood products: A comparison between x-ray scanning of logs and machine strength grading of lumber. *Forest Products Journal*, **55 (9)**, 55–60.

SS 230120, 2010: INSTA 142. Nordic visual strength grading rules for timber. Swedish Standards Institute, Stockholm, Sweden.

Part II

Paper I

Automated knot detection in computed tomography images of *Pinus sylvestris* L. and *Picea abies* (L.) Karst. using ellipse fitting in concentric surfaces

Authors:
Erik Johansson, Dennis Johansson, Johan Skog and Magnus Fredriksson

Reformatted version of paper originally published in:
Computer and Electronics in Agriculture.

© 2013, Elsevier Inc., reprinted with permission.

Abstract

High speed industrial computed tomography (CT) scanning of sawlogs is new to the sawmill industry and therefore there are no properly evaluated algorithms for detecting knots in such images. This article presents an algorithm that detects knots in CT images of logs by segmenting the knots with variable thresholds on cylindrical shells of the CT images. The knots are fitted to ellipses and matched between several cylindrical shells. Parameterized knots are constructed using regression models from the matched knot ellipses. The algorithm was tested on a variety of Scandinavian Scots pine (*Pinus sylvestris* L.) and Norway spruce (*Picea abies* (L.) Karst.) with a knot detection rate of 88-94 % and generating about 1 % falsely detected knots.

1 Introduction

Scanning equipment for sawlogs using X-ray technology is becoming increasingly common in sawmills. Such scanners are usually using two fixed X-ray sources, which is enough for detecting interesting internal log properties, such as knot whorl distance and heartwood content (Skog and Oja, 2009). A more detailed picture of the interior of logs can be constructed using computed tomography (CT), which results in a three-dimensional model of the log density distribution. Knot structure is one property amongst others that is seen in much more detail than when using discrete scanners with two fixed X-ray sources. Using a CT scanner, almost all knots can be traced from the pith to their end point. Historically, CT scanners have been constructed mainly for applications requiring relatively low feed speeds and not for scanning of logs in sawmills where speeds of 2 m/s are common. However, this is about to change since an industrial CT scanner managing these speeds is being developed within a European research project (Giudiceandrea et al., 2011). For such a scanner to be fully usable, it needs software capable of automatically extracting knot structure out of CT images.

There are several applications in which information of the knot structure from high speed CT scanning is valuable. One application is to rotate logs to their optimum position prior sawing in order to increase the value

of the sawn products. A study on Scots pine (*Pinus sylvestris* L.) by Johansson and Liljeblad (1988) showed a value increase of 9.6 % of the sawn timber when rotating logs to an optimum position with respect to knots and outer shape. That study evaluates square sawing and the optimum value is compared to horns down position, which is the commonly used rotational position. Another similar study on Scots pine (*Pinus sylvestris* L.) and Norway spruce (*Picea abies* (L.) Karst.) showed a potential value increase of 13 % compared to sawing logs horns down (Berglund et al., 2013).

Detailed knot data is also valuable at the log sorting station, where logs are measured and sorted into different piles depending on size, shape and quality. A study has shown that discrete X-ray scanning can be used to sort logs based on interior quality and this manner of sorting can be used to improve the quality of the sawn timber (Oja et al., 2005). It is reasonable to expect that by using more detailed knot data from a CT scanner, quality sorting can be more accurate.

In traceability applications, knot structure information from a CT scanner would also be valuable. (Flodin et al., 2008) presents a method to trace sawn boards from Scots pine (*Pinus sylvestris* L.) to the sawlog they originated from. By gathering lengthwise knot position in logs using a one way X-ray scanner, sawn boards could be traced to the correct log with 95 % accuracy. Since CT scanning generates more detailed knot information than a one way X-ray scanner, traceability should be even more accurate if using a CT scanner.

There are many articles (Andreu and Rinnhofer, 2003; Baumgartner et al., 2010; Grundberg and Grönlund, 1992; Hagman and Grundberg, 1995; Longuetaud et al., 2012; Nordmark, 2002) describing various kinds of algorithms that aim to extract knot data from images obtained using low speed CT scanning. Longuetaud et al. (2012) present a thorough review of papers on the subject as well as an algorithm using 3D connected components and a 3D distance transform. Another contribution is presented by Grundberg and Grönlund (1992), where the authors use concentric surfaces in the heartwood. In that part of sawlogs, knots have much higher density than surrounding wood. They can therefore be segmented by thresholding the concentric surfaces and using ellipse fitting on the resulting high density objects. In sapwood, knots are harder to detect since the density difference of knots and surrounding wood is small.

Grundberg and Grönlund (1992) approaches this problem by concentrating the search of each knot in the sapwood to a small area calculated with data from the corresponding heartwood knot. The authors show good results on Scandinavian Norway spruce (*Picea abies* (L.) Karst.) and Scots pine (*Pinus sylvestris* L.) logs.

Although there are many knot detection algorithms presented by other authors, none have been tested on images from high speed CT scanning. The aim of this study is to create an algorithm that can detect knots in high speed industrial CT images of Scandinavian Scots pine (*Pinus sylvestris* L.) and Norway spruce (*Picea abies* (L.) Karst.). Robustness is the main priority, which means maintaining a high detection rate and a small amount of falsely detected knots when using a wide spectrum of log samples. The algorithm presented in Grundberg and Grönlund (1992) has proven to be robust, which is why the algorithm presented in this article will use the main concepts described in Grundberg and Grönlund (1992).

2 Materials and methods

2.1 Logs and CT images

Logs used for validation come from the Swedish Stem Bank (SSB) (Grönlund et al., 1995), which consists of data from about 600 Scots pine (*Pinus sylvestris* L.) logs and about 800 Norway spruce (*Picea abies* (L.) Karst.) logs. Most logs in the SSB come from trees grown in Sweden, but smaller samples from France and Finland are also included. The logs were scanned with a medical CT scanner (Siemens SOMATOM AR.T) and the CT images are stored as 512×512 pixel cross sections every 10 mm. In this study, two datasets of CT images were chosen: dataset A and B, respectively. For dataset A, 10 Scots pine logs and 8 Norway spruce logs with varying properties and defects were chosen. The length of the logs varied from 3.6 to 5.2 m and the top diameter from 122 to 332 mm. Except from top diameter, the properties and features important for the selection of logs were heartwood content, heartwood shape, rot, top ruptures, density, knot structure and knot size. Dataset B consists of 47 Scots pine logs within a top diameter range of 150 to 303 mm and length in the interval 3.9 to 5.2 m. The logs are a subset of the logs used in a study (Grönlund, 1995) to validate calculations of dead knot border. In that study, the logs were cut

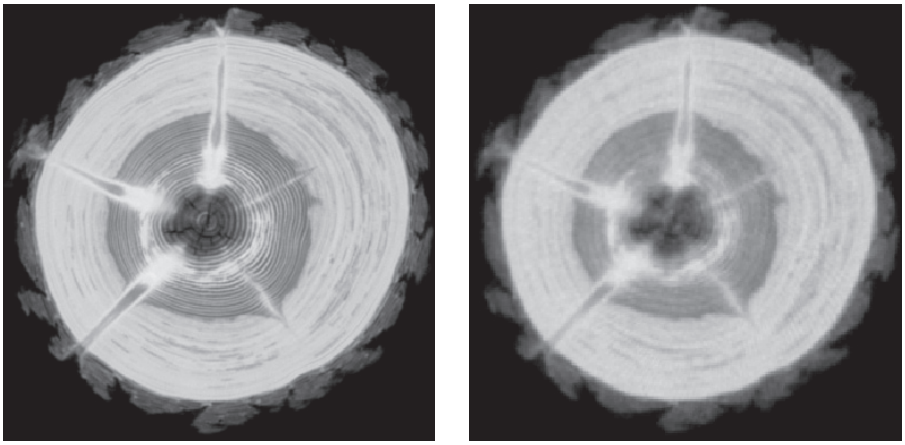

(a) Medical CT slice. (b) Simulated high speed CT slice.

Figure 1: A comparison of a slice from a medical CT scanner and the same slice reconstructed by simulating a high speed industrial CT scanner.

into boards and the dead knot border position was measured. The CT images in both datasets were processed with a simulation software to obtain images with quality equal to that of a high speed industrial CT scanner. This software is using the same CT reconstruction algorithm that will be used in such a scanner (Katsevich, 2004; Giudiceandrea et al., 2011). A comparison between an original CT cross section from the SSB and the corresponding simulated high speed image is shown in Figure 1.1(a) and 1.1(b).

2.2 Prerequisites

There are three main inputs to the knot detection algorithm: pith position, bark-wood border and sapwood-heartwood border. All data required were gathered automatically with software developed specifically for a high speed industrial CT scanner. The pith detection was performed using Hough transforms and is described by Longuetaud et al. (2004). Sapwood-heartwood and bark-wood border were found using a series of filters applied on polar images of the logs' CT images, where the polar images had their origin at the pith.

2.3 Concentric surfaces (CS's)

The knot detection algorithm uses something denoted as concentric surfaces (CS's). A CS is similar to a cylindrical shell, but with a major difference in how the radius is defined. Slightly simplified, the radius is defined so that the CS's approximately follow the annual rings of the log, instead of having a circular shape. In this paper, there are three different types of CS's used: log CS's, heartwood CS's and sapwood CS's. Those three types differs in which way the radius is chosen. Let $r_h(\theta, z)$ be the distance from pith to the heartwood-sapwood boundary, let $r_b(\theta, z)$ be the distance from the pith to the sapwood-bark boundary and let p be a parameter ranging from 0 to 1. θ and z are the angular and lengthwise coordinates in the log coordinate system. The different types of CS's have radii

$$r_{log} = pr_b(\theta, z) \tag{1}$$

$$r_{heart} = pr_h(\theta, z) \tag{2}$$

$$r_{sap} = r_h(\theta, z) + p\left(r_b(\theta, z) - r_h(\theta, z)\right). \tag{3}$$

Between CS's of the same type, the radii differs only due to a change in p value. An example of a heart CS is shown in Figure 1.3(a).

2.4 Algorithm description

The knot detection algorithm developed in this study is similar to the one presented in Grundberg and Grönlund (1992), although many aspects differs in order to obtain good results on relatively noisy high speed industrial CT images. Differences include, but are not limited to, how knots are thresholded in heartwood CS's, how ellipses in different CS's are matched to each other and how the dead knot border is calculated. When constructing this algorithm the main foci were stability and robustness rather than accuracy, i.e. the aim was to achieve a high knot detection rate and a low amount of falsely detected knots. The algorithm contains a collection of parameters, such as threshold values and filter lengths, all chosen to optimize the performance when running the algorithm on Scandinavian Scots pine and Norway spruce logs. In order to test the robustness of the algorithm, all parameters were the same for both Scots pine and Norway spruce when conducting validations. Figure 2 shows a flow chart with the

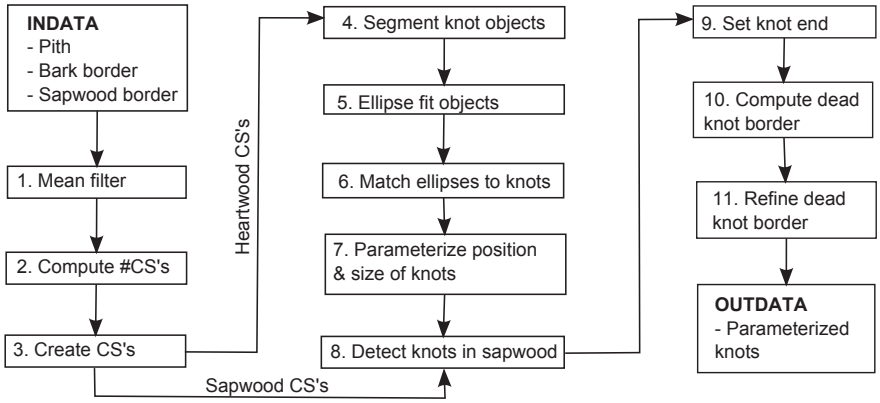

Figure 2: Flow chart of the main steps in the knot detection algorithm. Detailed descriptions of each step are found in section 2.4.

main steps in the algorithm. These steps are described in more detail in a list below.

1. Apply a 15 mm mean value filter in radial direction to remove density variation due to annual rings.

2. Compute the number of heartwood and sapwood CS's respectively The total number of CS's are 10 and the number of those that are heartwood CS's is at least 5, but this number increases with increasing heartwood content. Remaining CS's are sapwood CS's. By choosing a total of 10 CS's the performance is sufficient while the computational time is kept low. The reason why at least 5 CS's must be in the heartwood is that it is much harder to detect knots in the sapwood compared to the heartwood.

3. Create all CS's. Let each surface overlap $2 \times 30°$ in the angular direction, i.e. ranging from $-30°$ to $390°$. An example of a heartwood CS is shown in Figure 1.3(a).

4. Obtain the background of each CS by applying a 510×510 mm median filter. Since the CS's have a constant number of pixels in azimuthal direction the median filter width in that direction measured in pixels will vary depending on the distance to pith. Each heartwood CS is

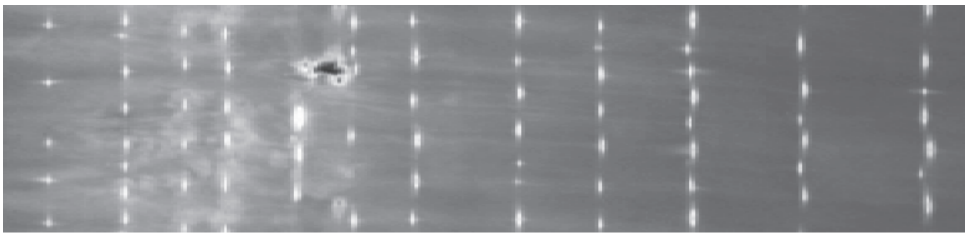

(a) Heartwood CS before applying knot segmentation.

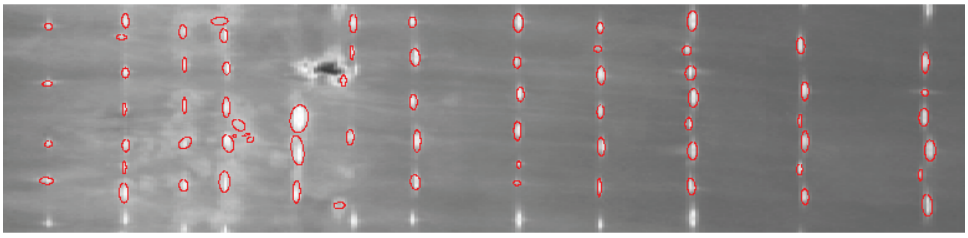

(b) Result of thresholding and ellipse fitting.

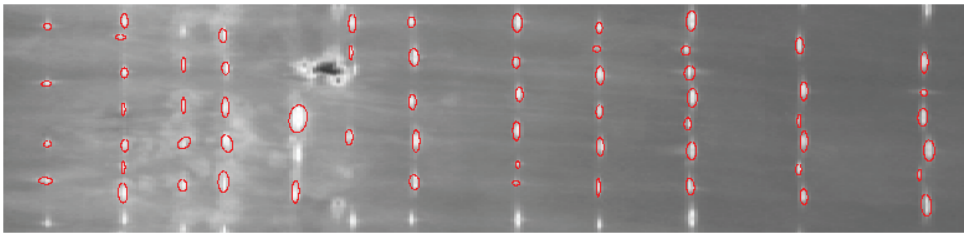

(c) Result of ellipse matching.

Figure 3: All three pictures show a heartwood CS of a pine log. Vertical axis is angular position and horizontal axis is lengthwise position. The angular axis is overlapping a total of 60° *and knots appearing twice in the pictures are only detected once (hence no ellipses for knots close to the edges). (a) shows the CS before running the knot detection algorithm. Each bright ellipse is most likely a knot. (b) shows all objects that are likely to be knots fitted to ellipses. In (c) some ellipses are removed because they could not be matched to ellipses in consecutive CS's.*

thresholded with a linear function of the background image of that CS. The threshold value at position (i, j) is $T_{i,j} = c_0 + c_1 B_{i,j}$, where $B_{i,j}$ is the background at position (i, j), c_0 and c_1 are constants. This thresholding segments objects representing areas of relatively high density compared to the background.

5. Fit all objects in all heartwood CS's to ellipses. Discard ellipses that either are too big or have the wrong orientation and also duplicates due to overlapping pixels of the CS, i.e. remove ellipses with centres outside $[0°, 360°)$. Figure 1.3(b) shows the result after this step.

6. For each ellipse in the innermost heartwood CS:

   6.1. Find an overlapping ellipse in the next heartwood CS that is sufficiently close and has a shape sufficiently similar. Repeat this procedure from the innermost CS to the one closest to the sapwood border. If no matching ellipse is found in two consecutive heartwood CS's then the knot is considered ended.

   6.2. Repeat step 6.1., but match ellipses from the heartwood CS closest to the sapwood to the one closest to the pith instead, i.e. instead of going away from the pith, go toward the pith. Only do this on ellipses that were not matched in step 6.1.

   6.3. All groups of matched ellipses that consist of less than three ellipses are deleted. All other ellipse groups are now called knots. After this step the result looks like Figure 1.3(c).

   6.4. Shrink all ellipse diameters by 20 % in order to adjust for overestimation when thresholding. The percentage was chosen because it set the mean errors of knot diameter for both spruce and pine close to zero.

7. Parameterize size and position of all knots using the regression models shown in Table 1. Figure 4 shows how size and position of knots are defined.

8. Track the knots through the sapwood by repeating for each knot:

   8.1. For each concentric surface in the sapwood starting at the one

closest to the pith:

8.1.1. Extrapolate the knot to the current concentric surface using the knot parameters.

8.1.2. Create a sub image with its center in the expected knot center with height 3 times knot diameter and width 2.5 times knot diameter. These factors produce an image big enough to be certain that the knot is included. They are kept as small as possible to get low computational time.

8.1.3. Calculate the standard deviation of each row and column in the sub image. If the maximum standard deviations of the rows and columns exceed 3 and 2.5 respectively, then a knot is considered to exist in the sub image.

8.1.4. If no knot is detected and there was no knot in the preceding concentric surface then the knot has ended. If so, continue with the next knot. If a knot was located in the previous surface, then continue with the next surface.

8.1.5. If a knot was found, try to find the position and size of it in the sub image using morphological dilation. This succeeds for the subset of knots that have higher density than the surrounding sapwood. Knots only distinguishable by difference in texture will not be found.

8.1.6. If no knot was found with the dilation method then use the parameterization data to create an ellipse.

8.1.7. Update the parameterization of the knot.

9. Set knot end for each knot in the following way: Let CS_{end} be the outermost CS where the knot was detected. Then set the knot end point for that knot at the intersection of the knot axis and a surface lying equidistant from CS_{end} and CS_{end+1}. A special case is if CS_{end} is the CS closest to the outer surface of the log. In this case, set the knot end to where the knot is expected to intersect the bark-wood border.

Table 1: Knot parameterization models. $A, B, \ldots, I$ are the parameters that are unique for each knot. All parameter models are first presented in Grönlund et al. (1995) except lengthwise position, which is described by Andreu and Rinnhofer (2003).

Knot diameter (rad)	$\phi(r) = A + Br^{1/4}$
Lengthwise position (mm)	$z(r) = C + D\sqrt{r} + Er$
Angular position (rad)	$\omega(r) = F + G\ln(r)$
Knot end (mm)	H
Dead knot border (mm)	I

10. Set dead knot border for each knot to the position where the knot has maximum size measured in mm. This is calculated from the derivative of the parameterized knot size. If there is no local maximum, then the whole knot is regarded sound.

11. Remove outlying dead knot border measurements using a regression model:

$$R(z) = c_0 + c_1 z, \tag{4}$$

where $R(z)$ is the regression line of the dead knot measurements along the lengthwise direction of the log. A residual is calculated for each measured dead knot border and a standard deviation of the residuals is calculated. All measurements with residual higher than two standard deviations are moved to the regression line.

2.5 Reference measurements

For dataset B, reference measurements on dead knot border were done on physical boards in another study (Grönlund, 1995) and no additional measurements were done in this study. Reference measurements in dataset A were made in high quality CT images and aimed to enable validation of knot geometry including size, position and end point. The actual measuring in dataset A was done by drawing ellipses around knots in log CS's

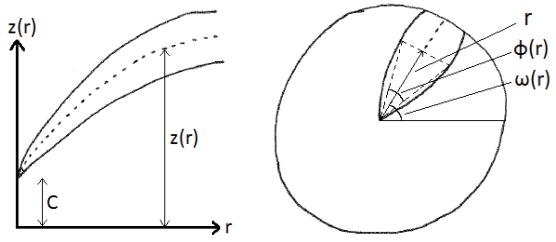

(a) Knot lengthwise position.

(b) Knot angular position and size.

Figure 4: (a) is showing how lengthwise position, $z(r)$, of the knot axis (dotted line) is defined as a function of the distance from pith, r. $z(r)$ is measured in the log's coordinate system. The constant, C, is the distance from the bottom of the log to the start of the knot. In (b), the definitions of knot angular position, $\omega(r)$, and knot diameter, $\phi(r)$, are described. Both are angles that varies for different values of r.

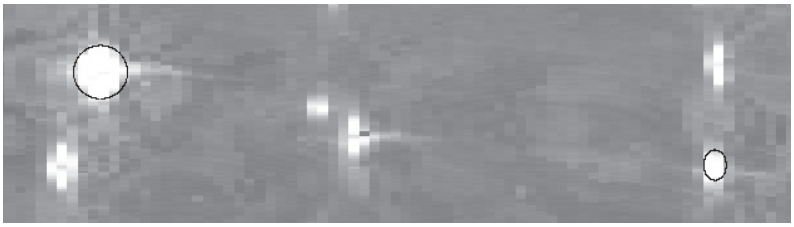

Figure 5: Two examples on how the ellipses used as reference measurements were drawn on a log concentric surface for data set A. The two ellipses are located in the upper left and lower right of the image. Ellipses should as far as possible overlap the highest density area. Only part of a concentric surface is shown.

(described in section 2.3) as showed in Figure 5. Ellipses for each non-occluded knot were drawn at radii corresponding to p-values of 0.2, 0.3, ..., 0.9 in equation (1). This yields a total of eight ellipses per knot from the pith to the bark-wood border. Figure 6 visualizes the reference measurements from another view. For occluded knots, ellipses were drawn to the knot end point, which was marked with a single point. 127 knots for pine and 119 knots for spruce were measured and the number of measured knots per log varied from 9 to 21. Variety of different knot characteristics (size, end point, density and shape) was important when choosing the set of knots. Since density images did not give sharp knot borders, it was hard

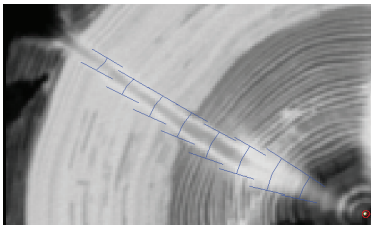

Figure 6: This image shows a part of a CT slice with a knot. The lines perpendicular to the radial direction correspond to the resulting reference measurements done in log CS's as showed in Figure 5.

to give the ellipses the correct size and therefore a measurement error was present. Knot size in sapwood was even harder to determine, but good estimates were possible to achieve. To reduce this error, the knot size were parameterized using the same regression model for diameter presented in Table 1. The knot center is well defined for the reference measurements and did not require further processing. End of each occluded knot was calculated as the distance from pith to exactly the midpoint of the last drawn ellipse and the next CS (where the knot disappeared). End of non-occluded knots was set to the intersection between the bark-wood border and the knot axis.

2.6 Evaluation of results

For data set A, the automatically detected knots' diameters and both lengthwise position and angular position of the knots' centres were compared to the reference measurements. This was done at the positions of the drawn manual ellipses, which means up to eight comparisons per knot. Knot ends were compared for each manually drawn knot. Mean error, standard deviation of the residuals, root mean square error and R^2 values were calculated. Also the portion of reference knots detected and amount of false positives were measured. The number of false positives was counted by manual inspection.

Data set B was purely used to validate dead knot border measurements (i.e. distance from pith to the point where knots transforms from sound to dead). Analogous to data set A, mean error, standard deviation of the residuals, root mean square error and R^2 values were calculated. The

reference measurements were taken from Grönlund (1995) and since that study only included Scots pine, dead knot border validation of Norway spruce has not been done within this study.

3 Results

The knot detection algorithm was run on both datasets and the resulting knots were compared to the reference measurements. Table 2 shows the results from accuracy measurements of knot geometry, knot end and dead knot border. A positive mean error means that the algorithm overestimates the knot feature. Diameter validation was done for three different size classes: small (< 10 10 mm), medium (10-20 mm) and big knots (> 20 mm). Figure 7 shows scatter plots of diameter, knot end and dead knot border. In the knot diameter scatter plot for spruce (Figure 1.7(b)), some individual knots generate interesting arc patterns that deviate much from the $y = x$ line. It is clear from Figure 1.7(c) and 1.7(d) that knot end often is underestimated for both species.

There were a total of 127 manually measured reference knots for Scots pine and the algorithm found 119 (93.7 %) of those. The respective numbers for Norway spruce were 119 reference knots and 105 (88.2 %) detected. A total of 795 knots for pine and 1095 knots for spruce were detected by the algorithm (79.5 and 137 knots per log for pine and spruce respectively). There were 8 false positives in total for pine and 6 of those were small (around 10 mm diameter or smaller). This means that 1.0 % of all found pine knots are false positives. Tests on spruce yielded 10 false positives (0.91 % of all detected knots) whereof 2 were small. Worth noting is that for pine, 20 % of the logs (2 logs) contributed with 75 % of the false positives. For spruce, the corresponding numbers were that 12.5 % (one log) gave 70 % of the false hits.

4 Discussion

4.1 Performance

With only about 1 % of all found knots being false positives the algorithm is robust, which was the main objective. The algorithm found between

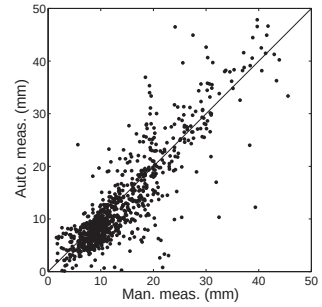

(a) Knot diameter pine

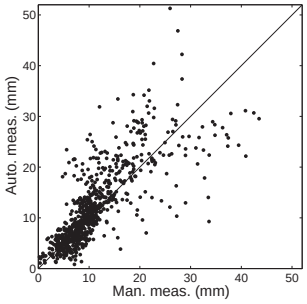

(b) Knot diameter spruce

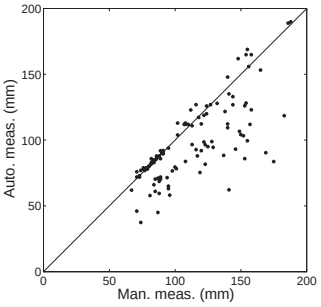

(c) Knot end pine

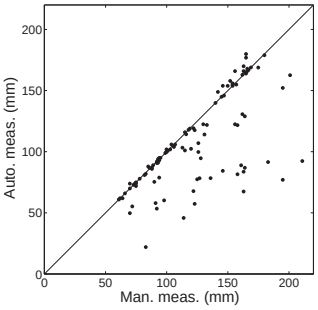

(d) Knot end spruce

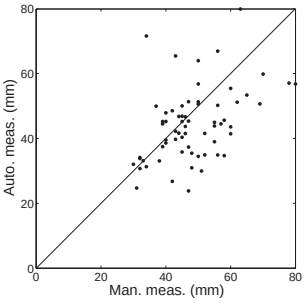

(e) Dead knot border pine

Figure 7: Scatter plots for pine and spruce validation data. The lines correspond to $y = x$.

Table 2: Error measurements on knot diameter, knot position, knot end and dead knot border. The knot diameters are presented in total, but also in three different size classes. Diameter ranges for the size classes in column 2 are all in mm. Denotations for knot lengthwise position, knot angular position and dead knot border are z position, ω position and DK border, respectively. R^2 values for knot position were omitted because they had meaningless statistical interpretation. Validation of dead knot border for spruce was not included in this study and was intentionally left blank to clarify this.

Species	Knot feature	Mean error	SD of error	RMSE	R^2	Sample size
Pine	Dia (0,10) (mm)	-1.1	2.4	2.6	0.26	340
Pine	Dia [10,20) (mm)	-1.2	4.9	5.0	0.35	340
Pine	Dia [20,∞) (mm)	0.035	7.1	7.1	0.47	141
Pine	Dia total (mm)	-0.93	4.6	4.7	0.75	821
Pine	z position (mm)	-2.6	9.2	9.5	-	784
Pine	ω position (°)	0.34	2.3	2.4	-	784
Pine	Knot end (mm)	-14	21	25	0.55	119
Pine	DK border (mm)	-4.0	12	12	0.19	65
Spruce	Dia (0,10) (mm)	0.64	3.3	3.4	0.33	437
Spruce	Dia [10,20) (mm)	3.1	5.3	6.1	0.46	225
Spruce	Dia [20,∞) (mm)	-4.1	8.2	9.2	0.20	72
Spruce	Dia total (mm)	0.93	5.1	5.1	0.60	734
Spruce	z position (mm)	-0.93	7.8	7.9	-	717
Spruce	ω position (°)	-0.19	1.9	1.9	-	717
Spruce	Knot end (mm)	-16	29	33	0.49	105
Spruce	DK border (mm)	-	-	-	-	0

88 % and 94 % of all reference knots, which is a high number keeping in mind the low rate of false positives. In the software development stage, there was a fine line between finding more knots introducing false positives and decreasing false positives finding fewer knots. Bad pith detection due to top ruptures and rot in the heartwood were the main reasons for false positives.

The random errors in measuring z-position were 9.2 mm and 7.8 mm for pine and spruce, respectively. These values are low since they are less than the z-resolution of the CT images, which is 10 mm. In the case of angular position, the achieved random errors of about 2° is low compared to a typical rotation positioning error in a saw-line of 5°.

Automatic measurements of knot end have relatively high errors. Figure 1.7(c) and 1.7(d) show that the problem is underestimation, which

is due to insufficient knot detection in sapwood. The algorithm has a tendency to lose track of knots in the sapwood because of small contrast between knots and surrounding wood. Therefore, steps 8.1.2 to 8.1.6 in section 2.4 need improvement to get more accurate knot end measurements. For occluded knots, the resolution of knot end measurements is the distance between the concentric surfaces. Additional CS's would therefore increase the resolution and decrease the error.

A study on Scots pine (*Pinus sylvestris* L.) by Grundberg (1999) presents how various error levels on knot diameter and dead knot border affect estimated product value. According to that study, a random error of 10 mm in dead knot border and 6 mm in maximum knot diameter (which is roughly what was achieved in this article) generate a product value 6.5 % lower than the reference value with no errors. If the error in diameter is decreased to 3 mm, the value difference becomes 1.7 %. When doing the opposite; keeping diameter error at 6 mm and decreasing dead knot border error to 5 mm, the value difference becomes 6.3 %. Improved diameter measurements would therefore benefit the algorithm more than improved dead knot border calculations.

It can be concluded that, at least for Scots pine, future work should prioritize improvements in knot size measurements. Species should be kept separate in future work due to differences in knot appearance between species. In this study, the same parameters were used on both pine and spruce with purpose to create a robust method that would work for both species. Using different parameters on different species would generate higher accuracy. Dead knot border is closely related to maximum knot diameter (Grönlund, 1995) and improvements in knot diameter measurements would increase the accuracy of detecting dead knot border.

4.2 Error sources

In the reference measurements described in section 2.5, knot center position is well defined and the errors in the reference measurements should be insignificant. On the other hand, reference measurements of knot size have a random error due to non-sharp density boundaries around knots in the CT images. This is true especially for measurements made in the sapwood. However, most reference measurements were done in the heartwood and a regression model was used to lower the measurement error.

Therefore, the measurements in the heartwood indirectly improve the sapwood measurements. It can be expected that the reference measurements of knot diameter are accurate enough to validate the algorithm.

Another issue with the knot size reference measurements is that it is unclear exactly how large a knot is given the density distribution. Systematic errors in the reference measurements are therefore present, but the random errors should be unaffected. The relation of knot size and density distribution should be evaluated in future studies. Then the results of this paper can be adjusted accordingly.

Knot end was hard to locate accurately with the human eye in the CT images and there are likely significant errors in those reference measurements. That part of the validation should be seen in a rough sense. A destructive sampling of knot end would improve this.

Dead knot border reference measurements were done on physical boards and can be expected to be accurate.

4.3 Comparison to algorithms presented in other articles

The accuracy of the algorithm presented in this article cannot be directly compared to algorithms described by other authors for two reasons. First and foremost, the algorithm in this paper is designed for an industrial high speed CT scanner (Giudiceandrea et al., 2011). There are no other articles presenting algorithms designed for that purpose. Therefore, the CT images used in this study are of lower quality compared to images used in other studies, which are of better quality (Grundberg, 1999; Longuetaud et al., 2012; Oja, 1997, 2000). Second, often the accuracy is measured in a different way, which makes comparisons difficult. However, comparisons will give a rough picture of the performance of the knot detection algorithm presented in this article.

A similar algorithm is described in Grundberg and Grönlund (1992) and is evaluated in Grundberg (1999), Grönlund (1995), Oja (1997) and Oja (2000). The errors in knot size, dead knot border and knot end are smaller than in this study while the errors of knot position in both lengthwise and angular direction are higher for Grundberg and Grönlund (1992). Number of false positives was similar between the two algorithms, but Grundberg and Grönlund (1992) achieved a slightly higher knot detection

rate. Two points must be considered when comparing the results and the first one, as stated before, is that this study used CT images of lower quality. The second point is that the pith detection in Grundberg and Grönlund (1992) was done manually and therefore is more accurate than the automatic method used in this study. Manual pith detection generates more predictable concentric surfaces and therefore do not the knot detection algorithm require the same robustness as if an automatic pith detection would have been used.

Longuetaud et al. (2012) describes a knot detection algorithm, which was tested on 7 dried square beams of silver fir (*Abies alba* Mill.) and Norway spruce (*Picea abies* (L.) Karst.). A detection rate of 85 % and a random error of knot maximum diameter of 2.9 mm could be reached. The detection rate is slightly lower but the accuracy in diameter measurements is higher than what is achieved in this study. Keep in mind that the CT images in the study of Longuetaud et al. (2012) are of higher detail and, more important, the beams were dried out which makes knot detection much easier. No direct conclusions can therefore be drawn from the comparison, but the approach of Longuetaud et al. (2012) would be interesting to test on the material used in this study.

5 Conclusions

- This article is the first to present a knot detection algorithm designed and validated for a high speed industrial CT scanner.
- The algorithm for detecting knots in high speed industrial CT images is robust in regard to low amount of false positives and a high detection rate when testing on a wide spectrum of logs.
- Accuracy of the algorithm is slightly lower than similar algorithms presented by other authors. However, due to differences in validation method and lower CT image quality in this study, no direct comparison is possible.

6 Acknowledgements

We would like to thank the people at Microtec for providing the reconstruction software used for simulating the high speed CT images. Also, we want to thank Microtec and Forstliche Versuchs- und Forschungsanstalt Baden-Württemberg for fruitful discussions and general help with software development.

References

Andreu, J.-P. and A. Rinnhofer, 2003: Modeling of internal defects in logs for value optimization based on industrial CT scanning. *Fifth International Conference on Image Processing and Scanning of Wood*, A. Rinnhofer, Ed., Bad Waltersdorf, Austria, 141–150.

Baumgartner, R., F. Brüchert, and U. Sauter, 2010: Knots in CT scans of Scots pine logs. *The Future of Quality Control for Wood & Wood Products*, D. Ridley-Ellis and J. Moore, Eds., Edinburgh, Scotland, The Final Conference of COST Action E53.

Berglund, A., O. Broman, A. Grönlund, and M. Fredriksson, 2013: Improved log rotation using information from a computed tomography scanner. *Computers and Electronics in Agriculture*, **90**, 152–158, doi: 10.1016/j.compag.2012.09.012.

Flodin, J., J. Oja, and A. Grönlund, 2008: Fingerprint traceability of sawn products using industrial measurement systems for x-ray log scanning and sawn timber surface scanning. *Forest Products Journal*, **58 (11)**, 100–105.

Giudiceandrea, F., E. Ursella, and E. Vicario, 2011: A high speed CT scanner for the sawmill industry. *17th International nondestructive testing and evaluation of wood symposium*, F. Divos, Ed., Sopron, Hungary.

Grönlund, A., L. Björklund, S. Grundberg, and G. Berggren, 1995: Manual för furustambank. Tech. Rep. 19, Luleå tekniska universitet, Luleå. In Swedish.

Grönlund, U., 1995: Quality Improvements in Forest Products Industry. Ph.D. thesis, Luleå University of Technology.

Grundberg, S., 1999: An X-ray LogScanner – a tool for control of the sawmill process. Ph.D. thesis, Luleå University of Technology, Luleå, Sweden.

Grundberg, S. and A. Grönlund, 1992: Log scanning – extraction of knot geometry. *The first international seminar/workshop on scanning technology and image processing on wood*.

Hagman, P. and S. Grundberg, 1995: Classification of Scots pine (*Pinus sylvestris*) knots in density images from CT scanned logs. *European Journal of Wood and Wood Products*, **53**, 75–81.

Johansson, L. G. and Å. Liljeblad, 1988: Some applications within the project "Quality simulation of saw Logs". Tech. rep., Tråtek. In Swedish with English summary.

Katsevich, A., 2004: An improved exact filtered backprojection algorithm for spiral computed tomography. *Advances in Applied Mathematics*, **32 (4)**, 681–697, doi:10.1016/S0196-8858(03)00099-X.

Longuetaud, F., J.-M. Leban, F. Mothe, E. Kerrien, and M.-O. Berger, 2004: Automatic detection of pith on CT images of spruce logs. *Computers and Electronics in Agriculture*, **44 (2)**, 107 – 119, doi: 10.1016/j.compag.2004.03.005.

Longuetaud, F., F. Mothe, B. Kerautret, A. Krähenbühl, L. Hory, J. Leban, and I. Debled-Rennesson, 2012: Automatic knot detection and measurements from X-ray CT images of wood: A review and validation of an improved algorithm on softwood samples. *Computers and Electronics in Agriculture*, **85 (0)**, 77–89, doi:10.1016/j.compag.2012.03.013.

Nordmark, U., 2002: Knot identification from CT images of young *Pinus sylvestris* sawlogs using artificial neural networks. *Scandinavian Journal of Forest Research*, **17**, 72–78.

Oja, J., 1997: A comparison between three different methods of measuring knot parameters in *Picea abies*. *Scandinavian Journal of Forest Research*, **12 (3)**, 311–315, doi:10.1080/02827589709355415.

Oja, J., 2000: Evaluation of knot parameters measured automatically in CT-images of Norway spruce (*Picea abies* (L.) Karst.). *European Journal of Wood and Wood Products*, **58 (5)**, 375–379.

Oja, J., B. Källsner, and S. Grundberg, 2005: Predicting the strength of sawn wood products: A comparison between x-ray scanning of logs and machine strength grading of lumber. *Forest Products Journal*, **55 (9)**, 55–60.

Skog, J. and J. Oja, 2009: Heartwood diameter measurements in *Pinus sylvestris* sawlogs combining x-ray and three-dimensional scanning. *Scandinavian Journal of Forest Research*, **24 (2)**, 182–188.

Paper II

Rotating *Pinus sylvestris* sawlogs by projecting knots from computed tomography images onto a plane

Authors:
Magnus Fredriksson, Erik Johansson and Anders Berglund

Reformatted version of paper submitted to journal.

© 2013, Magnus Fredriksson, Erik Johansson and Anders Berglund

Abstract

In this paper, a method for utilizing knot information from computed tomography (CT) scanning of Scots pine (*Pinus sylvestris* L.) logs is evaluated. The background for evaluating the method is the fact that a high speed industrial CT scanner is being developed, which will enable scanning of logs in sawmills at production speed. This calls for the possibility to optimize breakdown parameters in a fast way, since there are many decisions to be made and the timeframe for this is short. One of the important breakdown parameters is in which rotational position to saw a log.

The presented method used CT-data to create a two dimensional projection of knot information from a log, in order to minimize the amount of data to analyze. The center of gravity of the knot projection relative to the sawing pattern center was chosen as the rotational position of the log. The aim was to put large knots on the flat surfaces of the boards, since knots on edge surfaces have a more negative effect on board quality in the sorting rules used in this study. The method was tested by sawing simulation and was compared with the industrial praxis of sawing logs horns down. The results show an increase in board quality and value, albeit for a selected group of logs. The method is very sensitive to positioning errors, and thus not industrially feasible.

1 Introduction

In the sawmill industry, one long-withstanding dream is to be able to see the inside of logs, and to choose how to break them down individually, based on the internal wood structure. This has to some extent been realised by X-ray technology developed for and used in sawmills (Oja et al., 1998; Grundberg, 1999; Oja, 1999). However, the X-ray scanning technology employed today is based on a limited number of scan directions, which means that the available information of internal wood features is restricted. One or two scan directions means that the information available is a two dimensional image of the log, as opposed to three dimensional information of the wood structure. Not much can be said about for instance the position of knots, in the rotational direction, based on discrete X-ray scanning.

The commercial X-ray solutions available today are mainly based on discrete X-ray scanning, such as those supplied by RemaControl (two scanning directions), Bintec (one to six directions) and Microtec (two or four directions).

1.1 Possibilities for rotational position optimisation

Today however, other possibilities to scan saw logs in real time using X-ray are being realised, and a high speed scanner based on computed tomography (CT) technique is being developed and used in sawmills (Giudiceandrea et al., 2011). Various industrial prototypes for CT scanners are described by Wei et al. (2011). This will enable detection of for instance knots and their position in logs. When this information is available it will be possible to optimise the rotational position of a log when sawing, in order to improve value and quality of the sawn timber. Hodges et al. (1990) shows that an investment in CT scanning equipment should be profitable at least for large sawmills with a few percent increased value of the sawn goods, depending on various economical circumstances. Their study was made at hardwood mills in southern United States.

A rotational position optimisation will in most cases change the industrial praxis of today, which is to saw logs in the horns down position. "Horns down" means that the crook of the log is directed upwards during sawing. The optimal rotational position is subject to some uncertainty though, both in the detection of knots and in the precision with which it's possible to rotate a log in the sawing process. The effect of this lack of precision in the rotational position has been shown by Berglund et al. (2012). In their study, the value loss when failing to rotate logs properly was more than 50 %. Rotational errors can therefore seriously hamper attempts to optimise rotational position with respect to value of the sawn timber.

1.2 Previous work

It has been shown in earlier research (Lundahl and Grönlund, 2010) that it is possible to increase recovery in the breakdown process of logs by several percent, by choosing a rotational position which is different from horns down. For individual logs this number is even higher. This study was

made on Scots pine (*Pinus sylvestris* L.), and for Swedish sawmills and quality sorting rules. A study on a similar material made by Berglund et al. (2013), indicate a potential value increase of about 13 %, when optimising rotational position and comparing to horns down. Another study, by Todoroki and Rönnqvist (1999), indicated a potential value increase of 16 % when practising live sawing and optimising sawing parameters. The study was made on Radiata pine (*Pinus radiata* D. Don). Finally, Rinnhofer et al. (2003) shows that it is possible to gain value by CT scanning logs and make decisions on the breakdown according to the CT images. They used a manual method for choosing the breakdown strategy. Among several tools used to aid the decision of the breakdown strategy, a projection of defects onto one plane was employed.

1.3 Problem statement

In order to realise an optimal rotational position there are other factors to consider than the scanning technology alone. Once the knots and other internal features of a log have been detected, a sawing strategy must be decided based on this information. This can involve rotational position as well as parallel displacement of the log, skewing, and choice of sawing pattern. Furthermore, possible secondary processing operations on the sawn product could be considered in this decision making. To automatically optimise all of these parameters based on simulation alone is computationally expensive, which is a problem in an on-line application. Therefore, a method capable of finding an optimal or close to optimal rotational position based on internal log features, in a faster way than testing all rotational positions through simulation, would be beneficial. It could save computational time which can be used for finding for instance an optimal parallel displacement of the log, or choosing an optimal sawing pattern. The hypothesis is that a log rotational position resulting in larger profit than horns down can be found, by projecting knots and other defects onto a plane, similar to the method used by Rinnhofer et al. (2003). This reduces the amount of information which needs to be processed, which potentially saves computation time. However, such a method might be susceptible to positioning errors, since it is based on a smaller amount of information than in Berglund et al. (2013). No industrially viable solution will be developed in this study, which can be seen as a feasibility study.

The study will be limited to Scots pine (*Pinus sylvestris* L.) and a production setup similar to that of Swedish sawmills.
The objectives of this study was to:

- Present a method of determining log rotational position in breakdown, based on CT scanned logs with detected knots, and the projection of these onto a plane.
- Investigate, by using sawing simulation, whether the presented method improves quality and value recovery for sawn timber, compared to sawing all logs horns down.
- Add errors both in the rotational position of the log and in the knot detection from CT scanning, and analyze the effect of the two respective errors on the presented method.

2 Materials and methods

2.1 The Swedish Pine Stem Bank

This study was based on 628 Scots pine (*Pinus sylvestris* L.) logs from the Swedish Pine Stem Bank (SPSB). The stem bank trees, from well-documented sites at different locations in Sweden, have been documented thoroughly regarding both tree properties and silvicultural treatments, felled, and bucked into logs. The logs have been scanned with a medical CT scanner (SOMATOM AR.T, Siemens AG, Forchheim, Germany) in order to record internal properties such as knots, pith location, and sapwood/heartwood border (Grönlund et al., 1995). This means that the SPSB contains logs from the butt, middle and top of trees. Log top diameters range from 107 to 373 mm. The knots of the SPSB are stored in a parameterised form, described further by Grönlund et al. (1995); Nordmark (2005).

2.2 Sawing simulation software

The SPSB can be used for sawing simulation through the simulation software Saw2003, developed by Nordmark (2005). The CT scanned logs of the SPSB provide input. Saw2003 models a sawmill that uses cant sawing

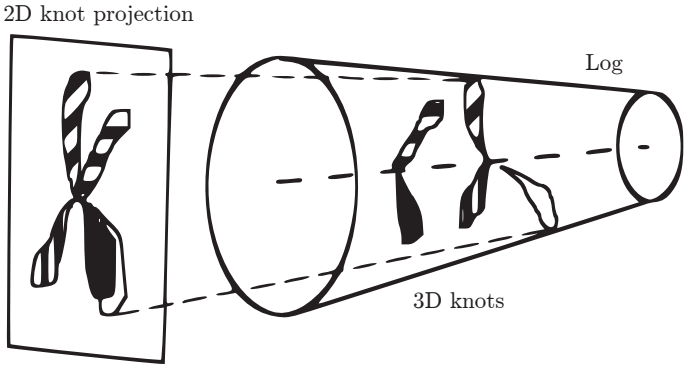

Figure 1: Projection of knots throughout a log onto a plane perpendicular to the log lengthwise direction. Knots are patterned to illustrate which knot that belongs to each projection.

with two sawing machines, with curve sawing in the second saw, edging and trimming. The latter two are value-optimised according to timber prices and grading criteria. Grading of the sawn boards in Saw2003 is done according to the Nordic Timber Grading Rules (Anon, 1997). Boards are graded into three quality classes, A, B or C, where A is the class with the strictest requirements. Grading in Saw2003 is based on knots and wane only, since other board features such as pitch pockets or rot are not represented in the SPSB. In these grading rules, knots on edges of boards are considered more severe than knots on the flat surface. The sawing simulation results in virtual boards with information about knots, value, dimensions and so forth. Saw2003 has been used extensively in earlier research (Chiorescu and Grönlund, 1999; Nordmark, 2005; Moberg and Nordmark, 2006; Lundahl and Grönlund, 2010).

2.3 Log rotation method with regard to knots

The choice of rotational position of each log was based on the azimuthal distribution of knots in the log. The parametrised knots of the SPSB log were projected onto a plane perpendicular to the longitudinal direction of the log (Figure 1). In a 256×256 image representing this plane, the value of each element was the sum of knot diameters in the projection direction. Thus, large knots had a larger weight in the projection, and several knots

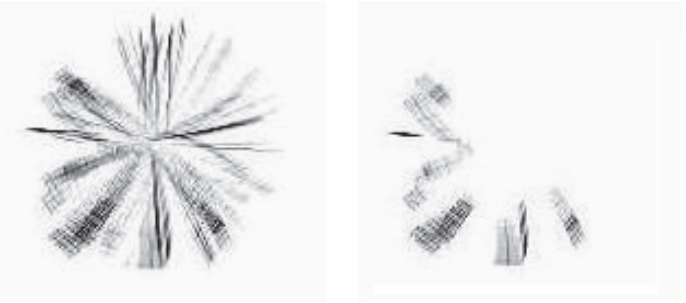

(a) Unfiltered knot projection (b) Filtered knot projection

Figure 2: Image representing projection of all knots through one log. Dark pixels represent high knot density and light pixels represent low knot density. Figure 2.2(a) shows a projection of all knots in a log, and Figure 2.2(b) shows the same projection after filtering out small knots and knot sections.

were added together. Furthermore, a dead knot was weighted according to Nordic Timber Grading Rules (Anon, 1997), by a factor of $\frac{1}{0.7}$. Thus, dead knots affect the projection to a higher degree than green knots. If a projected line from an image position through the log contained only clearwood, the element value was zero.

The final step of calculating the projection matrix was to filter out small diameter knots and knot sections. The threshold of this filter was automatically calculated individually for each log, as a linear function of the average knot diameter. This function was chosen by manually choosing a suitable knot diameter threshold for 30 of the logs, eliminating all but the six to ten largest knots. The exact number of knots that were kept depended on the size distribution of knots in the log. A linear regression function relating threshold diameter to average diameter was constructed for the 30 logs, $D_T = -8.5 + 103.4 \cdot D_m$, where D_T = threshold knot diameter in mm, and D_m = average knot diameter in pixels. This function was used for automatically filtering out knots in all logs in the SPSB. The projection matrix can be represented as an image, such as that in Figure 2, showing both the unfiltered and filtered matrix of one example log of the SPSB. In order to find the direction with the largest concentration of knots, the gravitational center of the projection matrix was calculated. The direction from the center of the sawing pattern towards the gravitational center was then chosen as the rotational position of the log, in an

attempt to turn the largest weight of knots towards the flat face of one of the center boards, thus avoiding large knots on edge faces.

2.4 Selection of logs

When the knot projection method was applied on the entire SPSB and the logs were sawn using simulation, the average value change for the sawn products of the logs was close to zero compared to sawing all logs horns down. Around half of the logs had an increased value and half of the logs had a decreased value.

For this reason, logs with a bow height of less than 14 mm and a difference between sawing pattern diagonal and top diameter of more than 18 mm was selected from the SPSB. The sawing pattern diagonal is the diagonal distance between corners in the outermost center boards in the sawing pattern, as illustrated in Figure 3. The bow height of the log is defined by the maximum distance between a line drawn through the centers of the log ends, and the log mid-line, as is shown in Figure 4. The reason for this selection was to avoid wane when rotating the logs from a different position than horns down. The limits were chosen with an exploratory approach where the combination of these limits, giving the highest value when rotating the log off the horns down position, was chosen. The limit on crook is consistent with the findings of Lundahl and Grönlund (2010). In the study, 10 of the 105 logs were not used since it was not possible to find a rotational position with the proposed method. This was due to the fact that the sawing pattern center and knot gravitational position coincided. This brought the total amount of tested logs down to 95, which is about $^1/_6$ of the total log population in the SPSB.

2.5 Testing the log rotation method through simulations

Saw2003 was used to evaluate the method of rotating logs according to the internal knot distribution. The sawing pattern for each log was chosen according to the top diameter, in a manner typical of Swedish sawmills. The corresponding sawing patterns for different top diameters are presented in Table 1. Since the sawing simulator employs value-optimised edging

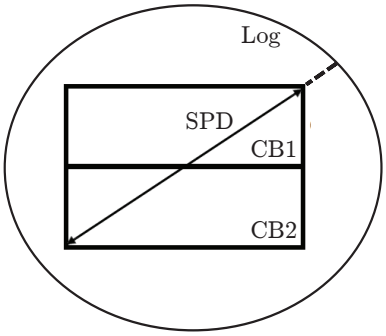

Figure 3: The sawing pattern diagonal (SPD), which is the diagonal distance between two corners of the outermost center boards in a sawing pattern. In this case there are only two center boards, CB1 and CB2, making these the outermost. The distance between sawing pattern diagonal and log top diameter is used as a selection parameter in this study, and is indicated by a short dashed line.

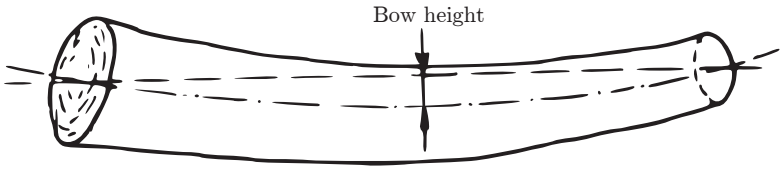

Figure 4: The definition of log bow height used in this study.

and trimming operations, the price of different board qualities 180 affects the simulation result. Therefore the prices used in this study are given in Table 2.

Comparison with sawing horns down

Sawing simulation was performed by sawing the 95 chosen logs of the SPSB horns down, as is the industrial praxis today. Then, the method of rotating logs towards the knot projection center of gravity was applied to the same logs, and the outcome in terms of value and quality of boards was compared between the two methods.

Table 1: List of sawing patterns used in this study. Lower limit = smallest top diameter allowed for logs within this sawing pattern. Upper limit = largest top diameter allowed for sawing pattern. Width = width of centreboards. Thickness = thickness of centreboards. All measurements are in mm. Sideboards are being edged to various sizes depending on value.

Lower limit mm	Upper limit mm	No. of centreboards	Width mm	Thickness mm
0	129	2	75	38
130	149	2	100	38
150	169	2	100	50
170	184	2	125	50
185	194	2	125	63
195	209	2	150	50
210	219	2	150	63
220	229	2	175	50
230	249	2	175	63
250	264	2	200	63
265	284	2	200	75
285	304	2	225	75
305	324	4	200	50
325	344	4	225	50
345	384	4	200	63
385	449	4	200	75

Table 2: Pricing of the qualities of sawn timber used in simulations, in Swedish crowns per cubic meter (SEK/m^3).

Quality	A	B	C
Centreboards	1850	1600	1000
Sideboards	3000	1400	1100

Comparison with a random rotational position

The knot projection method was also compared to a run of 30 simulations, were the log rotational position was randomized between 0 and 360 degrees, on the 95 test logs. The distribution of the average value difference when sawing logs in a random rotational position was then compared to the value obtained when sawing according to the knot projection

Adding a rotational error of 6 degrees

A similar comparison was made where a rotational error was introduced to both methods, an error which was normally distributed with a mean of 0° and a standard deviation of 6°. This error is at a level representative of the industrial situation. In this case no simulations using random rotational positions were made.

Adding an error in knot detection

Finally, an error in the representation of the knots in the sawing simulation was introduced. This was made in order to investigate the fact that automatic knot detection using CT scanning will not always be completely accurate. This test was made using three different levels of normally distributed, non-systematical errors to the detection of knot size, knot azimuthal direction and fresh knot length. The last refers to the distance between the pith of the tree and the dead knot border. The size of the standard deviations of these errors are presented in Table 3. The error levels were chosen based on earlier experience; the levels are within the same range as reported for an automatic knot detection algorithm by Grundberg (1999). When comparing these errors, the method of common random numbers (Law, 2007) was used. Simulations and comparisons of board value and quality was carried out for the three error levels, using horns down sawing as well as rotating the logs according to the knot projection. In this case, the SPSB knots were considered to be the ground truth and were used as reference.

Table 3: Size of error added in the three different levels, expressed as standard deviation of the normal distribution function the errors were randomly selected from for each knot.

Knot feature	Low error	Medium error	High error	Unit
Knot diameter	15	30	45	%
Knot rotational position	1	3	5	°
Fresh knot length	5	10	15	mm

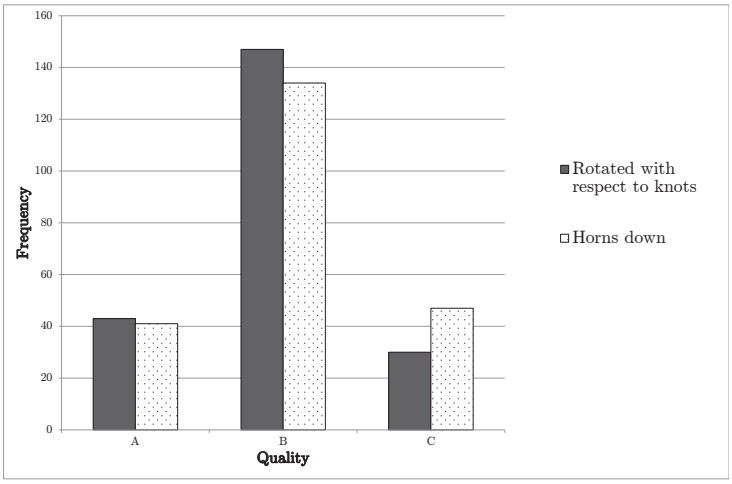

Figure 5: Distribution of board quality when sawing logs using knot projection (filled), and sawing logs horns down (dotted).

3 Results

3.1 Comparison with sawing horns down

For the 95 logs tested in this study, the average value change from sawing horns down compared to sawing based on the knots in the log, was +2.2 %. For 60 % of the logs, the value recovery was higher compared with sawing horns down. The quality distributions of the two compared methods, horns down and rotating according to knot orientation, are presented in Figure 5.

Table 4: Results of using the method on knots which were not detected properly. For all error levels, the quality distribution tended towards more A and B quality, and less C quality boards.

Error level	Low	Medium	High
Overall val. rec. diff. to horns down [%]	1.9	1.6	1.6
Share of logs with increased val. rec. [%]	59	51	58

3.2 Comparison with a random rotational position

The value potential distribution for the 30 runs when sawing in a random rotational position had a 95 % confidence interval, for the mean, of (1.43 %, 1.97 %). Since it was 30 independent, random test runs, the central limit theorem states that the distribution will be approximately normally distributed. This confidence interval can be compared to sawing the logs according to the knot projection, which resulted in a mean of 2.2 %, which is thus above the confidence interval of the random rotation value distribution. This value is located in between the 2^{nd} and 3^{rd} quartile of the random distribution.

3.3 Adding a rotational error of 6 degrees

When a rotational error was added to the sawing simulation of the 95 logs, the average value change was +1.3 % when sawing based on the knots, compared to horns down. 55 % of the logs showed an increased value recovery compared with sawing them horns down. The quality distributions for the two methods are shown in Figure 6.

3.4 Adding an error in knot detection

The results of using the proposed method, when the knots in the log are not properly detected, is presented in Table 4. The value recovery difference is expressed as the difference between sawing the logs horns down, and sawing them according to the knot projection, divided by the value when sawing horns down. The share of logs with increased value is the amount of logs with an increase in value compared to sawing horns down, divided by the total number of logs, which in this case was 95.

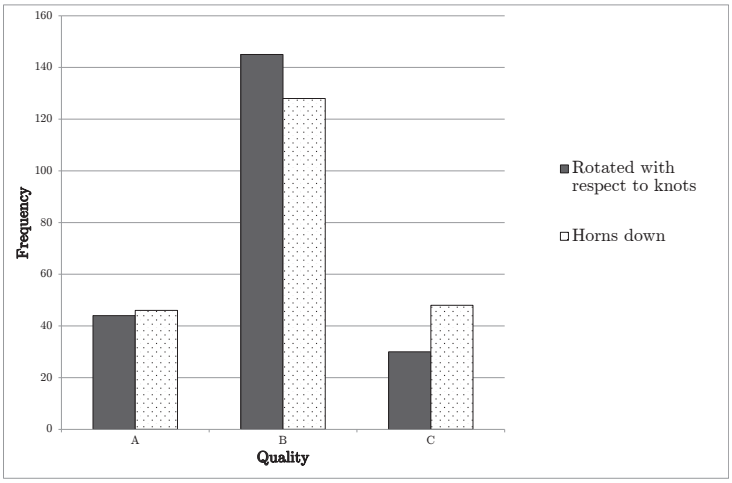

Figure 6: When adding a rotational error: Distribution of board quality when sawing logs using knot projection (filled), and sawing logs horns down (dotted).

4 Discussion

The proposed method improved the sawn board quality when comparing it to sawing horns down, for the 95 selected logs. It could also be shown that the value yield increased, compared to sawing the logs in a random rotational position. This increase was not very large compared to the potential shown in previous work, and the reasons for this could be several. The outer shape of the log was not accounted for in this method, apart from the fact that only logs with small bow and large difference between sawing pattern diagonal and top diameter was used. Furthermore, downgrading in the Nordic Timber Grading Rules is to a large degree affected by large knots and knots on the edge side of the board. This means that a small change in rotational position can have a severe effect on the value of the sawn timber, for instance when a large knot changes from being on the flat side of a board to the edge side. This sensitivity is shown by for instance Berglund et al. (2013). The rotational position of a log in some cases needs to be chosen with high precision, something which was not the case here. The method is thus sensitive to small errors. When

adding a rotational error which corresponds to the normal situation in many sawmills, the value increase was below the confidence interval of the mean when sawing in a random rotational position. When an error in the knot detection was added, this resulted in a value increase potential similar to that of introducing a rotational error in sawing.

Taking all results together, they show that the proposed method is not suitable for industrial use in its present shape. The sensitivity to errors is high, as shown by the simulation results. In the ideal case without errors, the quality of boards were changed to some degree towards the higher qualities.

The value increase of 2.2 % compared to sawing horns down was however so small, that it cannot be refuted that it was the result of pure chance. The value increase was above the confidence interval of the value distribution when sawing in a random rotational position, but still within the 2nd and 3rd quartile. It is also quite far from the potential shown by previous research (13 - 16 %).

It should be noted that the simulations made in this study was made on logs that were scanned with a medical CT scanner, which uses a different scanning principle and reconstruction algorithm than the industrial high speed scanner. The produced image stacks are however very similar, and the principle of the method proposed here should work on this type of data as well. The similarities are demonstrated by Giudiceandrea et al. (2011).

The material in this study was limited to Scots pine logs from Sweden, which means that the results should not be generalised outside this limitation. The SPSB contains logs from a large variety of growth conditions however, and should be sufficiently varied to account for a large part of the Swedish pine forest inventory. One should also bear in mind that the method was tested on a selection of logs in the SPSB, which corresponds to about $^1/_6$ of the entire population of logs. The reason for doing this was to reduce the effect of the outer shape of the log, since this is not accounted for in the projection method. The implication of this choice is however that the results presented here are only representative for a sample of selected logs. This means that in an industrial situation, a very restrictive log sorting would have to be done before using this projection method. A small amount of logs could be sawn by this method, and the rest horns down. However, this seriously limits the practical applicability

of this method.

When assessing the inner features of a log in an industrial situation, and adapting the breakdown strategy to these, there are many factors which need to be taken into account. One of the main advantages of the proposed method is that it assesses a projection of the information available in CT data, thus potentially decreasing computational time compared to a full optimisation. This is important in an industrial situation, where a breakdown decision needs to be made for each individual log, in a short timeframe. The saved computational time could be used for assessing translational position of the log, sawing patterns or other decisions related to the breakdown procedure.

Possible future work includes adding other defect types such as rot or pitch pockets to the data. These could be projected and weighted in the same manner as the knots, and in the case of these defects it is also desirable to turn the log so they end up on one half of the sawing pattern. The direction in which to rotate the logs could be more distinct in that case, but it is not certain. The effect of outer shape of the log should also be included.

5 Conclusions

It can be concluded from this study that the approach to automatically find a rotational sawing position from CT images by using projected information about knot positions throughout the log, shows some positive tendencies. For the log type studied, it improves the quality distribution and the value of the sawn timber, compared to sawing logs horns down. It should however be noted that the outer shape of the log has an effect on the value, and the results obtained here are only applicable for a sample of selected logs with a suitable shape. When testing the method using errors in knot detection and log rotation, corresponding to an industrial situation, the method showed a performance no better than chance. The sensitivity to errors is high, and this indicates that the method is not mature for industrial application in its current state.

References

Anon, 1997: *Nordic Timber: Grading rules for pine (Pinus sylvestris) and spruce (Picea Abies) sawn timber: Commercial grading based on evaluation of the four sides of sawn timber.* Föreningen svenska sågverksmän (FSS), Sweden.

Berglund, A., O. Broman, A. Grönlund, and M. Fredriksson, 2013: Improved log rotation using information from a computed tomography scanner. *Computers and Electronics in Agriculture*, **90**, 152–158, doi: 10.1016/j.compag.2012.09.012.

Chiorescu, S. and A. Grönlund, 1999: Validation of a ct-based simulator against a sawmill yield. *Forest Product Journal*, **50**, 69–76.

Giudiceandrea, F., E. Ursella, and E. Vicario, 2011: A high speed CT scanner for the sawmill industry. *17th International nondestructive testing and evaluation of wood symposium*, F. Divos, Ed., Sopron, Hungary.

Grönlund, A., L. Björklund, S. Grundberg, and G. Berggren, 1995: Manual för furustambank. Tech. Rep. 19, Luleå tekniska universitet, Luleå. In Swedish.

Grundberg, S., 1999: An X-ray LogScanner – a tool for control of the sawmill process. Ph.D. thesis, Luleå University of Technology, Luleå, Sweden.

Hodges, D. G., W. C. Anderson, and C. W. McMillin, 1990: The economic potential of ct scanners for hardwood sawmills. *Forest Product Journal*, **40**, 65–69.

Law, A. M., 2007: *Simulation Modeling and Analysis.* 4th ed., McGraw-Hill, New York, United States.

Lundahl, C.-G. and A. Grönlund, 2010: Increased yield in sawmills by applying alternate rotation and lateral positioning. *Forest Product Journal*, **60**, 331–338.

Moberg, L. and U. Nordmark, 2006: Predicting lumber volume and grade recovery for scots pine stems using tree models and sawmill conversion simulation. *Forest Product Journal*, **56**, 68–74.

Nordmark, U., 2005: Value recovery and production control in the forestry-wood chain using simulation technique. Ph.D. thesis, Luleå University of Technology, Luleå, Sweden.

Oja, J., 1999: X-ray measurement of properties of saw logs. Ph.D. thesis, Luleå University of Technology, Luleå, Sweden.

Oja, J., S. Grundberg, and A. Grönlund, 1998: Measuring the outer shape of pinus sylvestris saw logs with an x-ray logscanner. *Scandinavian Journal of Forest Research*, **13**, pp. 340–347.

Rinnhofer, A., A. Petutschnigg, and J.-P. Andreu, 2003: Internal log scanning for optimizing breakdown. *Computers and Electronics in Agriculture*, **41 (13)**, 7 – 21, doi:10.1016/S0168-1699(03)00039-5, developments in Image Processing and Scanning of Wood.

Todoroki, C. L. and E. Rönnqvist, 1999: Combined primary and secondary log breakdown optimisation. *The Journal of the Operational Research Society*, **50 (3)**, pp. 219–229.

Wei, Q., B. Leblon, and A. La Rocque, 2011: On the use of x-ray computed tomography for determining wood properties: a review. *Canadian Journal of Forest Research*, **41**, 2120–2140.

Paper III

Value optimized log rotation for strength graded boards using computed tomography

Authors:
Anders Berglund, Erik Johansson and Johan Skog

Reformatted version of paper submitted to journal.

© 2013, Anders Berglund, Erik Johansson and Johan Skog

Abstract

A possible application for an industrial computed tomography scanner in a sawmill is for finding an optimal rotational position of logs with respect to knots and outer shape. Since a computed tomography scanner is a great investment, it is important to investigate potential profitability of such an investment for different production strategies. The objective of this study was to investigate the potential value increase of the sawn timber of Norway spruce (*Picea abies* (L.) Karst.) by rotating logs to their optimum position prior sawing compared to sawing all logs in horns down position. The production strategy evaluated by log breakdown simulation in this case study was to produce strength graded timber of the center boards, while the side boards were appearance graded. This case study showed an average value increase with respect to the value of center boards, side boards and chips of 11%.

1 Introduction

An industrial CT scanner for the sawmill industry (Giudiceandrea et al., 2011) leads to questions regarding production strategies, and how to increase the profit return if making the investment of such a scanner. In earlier work (Berglund et al., 2013), log breakdown has been simulated for about 800 Norway spruce logs and 600 Scots pine logs from mainly Sweden and Finland, but also France. This made it possible to investigate the profitability in an improved log rotation when using a CT scanner in the saw line to optimize the rotational position. In the study, all sawn timber was appearance graded according to the Nordic timber grading rules (Anon, 1997).

Some sawmills produce and sell strength graded timber instead of, or in addition to, appearance graded timber and it would be useful to investigate the profitability of using a CT scanner in the saw line to optimize this breakdown process. Since internal features of logs, such as knots, can be detected, there should be a possibility for rotating logs to avoid edge knots and arris knots and thereby increasing the share of high strength boards.

When using timber in load-bearing constructions, strength and stiffness of the material have to be within ensured limits (Johansson, 2003).

The procedure is somewhat different when it comes to wood compared to other engineering materials such as steel or concrete, where strength and stiffness of the material more easily can be controlled. To control mechanical properties of wood and to ensure dimensional strength and durability of a construction, wood is graded according to grading rules. There are two methods under use to measure board strength, namely *visual strength grading* and *machine strength grading*.

Visual strength grading, as the name implies, ensures that the visible defects on a board does not exceed the limits specified by the grading rule. Visual strength grading in Scandinavia is performed either according to the Nordic standard (SS 230120), or alternatively according to the European standard (EN 14081-1). The Nordic standard pertains to Scots pine (*Pinus sylvestris* L.), Norway spruce (*Picea abies* (L.) Karst.), Sitka spruce (*Picea sitchensis* (Bong.) Carr.), Silver fir (*Abies alba* Mill.), Douglas fir (*Pseudotsuga menziesii* (Mirb.) Franco) and Larch (*Larix decidua* Mill., *Larix eurolepis*, *Larix kaempferi* (Lamb.) Carr.), while the European standard pertains to all hardwoods and softwoods. Timber graded according to these standards are sorted into classes T3, T2, T1 and T0 with corresponding strength classes C30, C24, C18 and C14. The numbers in the names of the strength classes correspond to bending strength in MPa.

For machine strength grading, the pieces are passed through a machine, which estimates the strength and stiffness of the pieces based on one or several non-destructively measured parameters. The grading rules applied to machine graded timber is the same all over Europe and is performed according to the European standard (EN 14081-1; EN 14081-2; EN 14081-3). The machine grading rules pertain to all hardwoods and softwoods for structural use.

The objective of this work was to investigate, by log breakdown simulations, how the log rotation affects the value outcome of visually strength graded timber according to the Nordic standard (SS 230120). The production strategy of this case study was from the perspective of a Scandinavian sawmill processing Norway spruce (*Picea abies* (L.) Karst.) to produce strength graded timber of the center boards, while the side boards are graded according to the appearance grading in the Nordic timber grading rules (Anon, 1997). The reason for grading the center boards by visual grading is that visual grading can be taken under consideration prior to

sawing using an industrial CT scanner since internal features like knots can be detected (Johansson et al., 2013).

2 Materials and methods

2.1 The European spruce stem bank

The material used in this study comes from the ESSB (Berggren et al., 2000), which consists of data from about 800 Norway spruce (*Picea abies* (L.) Karst.) logs. The logs origin from 31 plots in different geographic locations, where the largest share is from Sweden, but also plots from Finland and France are represented.

When collecting these logs, six trees were chosen in each plot; two in a lower diameter class, two in a middle diameter class and two in a larger diameter class. The stems were divided into the diameter classes based on the quadratic mean diameter at breast height of the stand, with class limits at half a standard deviation above and below this mean (Björklund and Moberg, 1999). The diversity of the logs in the ESSB with respect to diameter, outer shape and knot structure makes it a representative data set for logs in the Scandinavian countries, and thereby suitable for the objective of this study.

The logs were scanned using a medical CT scanner (Siemens SOMATOM AR.T) and the resulting CT images shows the log outer shape, as well as internal features such as pith location, heartwood border and knots. The knots are described by nine parameters specifying the knot geometry, position, and direction in the log (Oja, 2000). All logs were scanned every 10 mm and the resulting images of each CT slice had 512×512 pixels with 12 bit gray scale values.

The description of log outer shape and knots in the ESSB makes it possible to simulate log breakdown of these logs.

2.2 Log breakdown simulation

Log breakdown simulation has the advantage that it can be carried out in a relatively short time frame and the input data can be processed an infinite number of times. This makes relative studies possible by comparing different methods or strategies on the same material. These reasons have

made it widely used in the field of wood technology (Björklund and Julin, 1998; Todoroki and Rönnqvist, 1999; Nordmark, 2005).

In this work the SAW2003 software (Nordmark, 2005) was used since it is developed to interact with the data in the ESSB. The outer shape of the log is described by a CT slice every 100 mm whereas knots are described using full information from the CT images (every 10 mm). The sawing procedure is governed by the specified sawing patterns and prices of sawn timber.

Grading

The side boards were appearance graded with respect to the criteria for knots and wane specified in the Nordic timber grading rules (Anon, 1997) using SAW2003. These rules separate the boards into three different qualities, A, B and C. Boards not fulfilling either of these qualities are turned into chips.

The center boards were outputted from SAW2003 and strength graded and trimmed according to the visual grading described in the Nordic standard (SS 230120) using the software MATLAB version R2012b. Timber graded according to the Nordic standard is divided into sorting classes T3, T2, T1 and T0 with corresponding strength classes C30, C24, C18 and C14. The numbers in these strength class names correspond to bending strength in MPa.

The grading was simplified and only carried out with respect to knots and wane on the boards since these defects are most important for appearance graded and strength graded timber. Information regarding other wood features such as annual ring width, splits, rot, resin pockets, top rupture etc. was not accounted for. Additionally, for the strength grading according to SS 230120, an arris knot lying completely or partly within wane should according to the standard be measured as an edge knot, but it was still measured as an arris knot. No special consideration was given to splay knots occurring as a consequence of top rupture.

The strategy investigated in this study was to produce center boards of sorting class T3 or T2. The center boards that did not fulfil the quality demands of class T3 or T2 were sold at a lower price.

Table 1: The logs are sorted into a SC with respect to their top diameter. The first saw determines the width of the center boards and the thickness of the side boards in the first saw. The second saw determines the thickness of the center boards and additional side boards. All measures are nominal target values.

SC	Sawing pattern (mm)	Top diameter range (mm)	Post First saw (mm)	Post Second saw (mm)
1	38 by 100 by 2	130-149	19, 100, 19	19, 38, 38, 19
2	50 by 100 by 2	150-169	19, 100, 19	19, 50, 50, 19
3	50 by 125 by 2	170-184	19, 125, 19	25, 50, 50, 25
4	63 by 125 by 2	185-194	19, 125, 19	19, 63, 63, 19
5	50 by 150 by 2	195-209	19, 19, 150, 19, 19	19, 25, 50, 50, 25, 19
6	63 by 150 by 2	210-219	19, 19, 150, 19, 19	19, 25, 63, 63, 25, 19
7	50 by 175 by 2	220-229	19, 19, 175, 19, 19	19, 25, 50, 50, 25, 19
8	63 by 175 by 2	230-249	19, 19, 175, 19, 19	25, 25, 63, 63, 25, 25
9	63 by 200 by 2	250-264	19, 19, 200, 19, 19	25, 25, 63, 63, 25, 25
10	75 by 200 by 2	265-284	19, 19, 200, 19, 19	19, 25, 75, 75, 25, 19
11	75 by 225 by 2	285-304	19, 19, 225, 19, 19	19, 25, 75, 75, 25, 19
12	50 by 200 by 4	305-324	19, 25, 200, 25, 19	19, 25, 50, 50, 50, 50, 25, 19
13	50 by 225 by 4	325-344	25, 32, 225, 32, 25	25, 25, 50, 50, 50, 50, 25, 25
14	63 by 200 by 4	345-384	25, 32, 200, 32, 25	19, 25, 63, 63, 63, 63, 25, 19

Sawing patterns and prices

The sawing patterns used are shown in Table 1 where the logs, depending on their top diameter, were sorted into their respective sawing class (SC). The sawing techniques applied were cant sawing and curve sawing, which are typical for sawmills in the Scandinavian countries. Figure 1 illustrates cant sawing, where the first sawing machine cuts the log into side boards and a cant. The cant is then rotated by 90 degrees and cut by the second sawing machine into side boards and center boards. The sawing allowance, e.g. shrinkage as well as deviations in the sawing, was set at 4% of the nominal width for each board dimension and the saw kerf width was set to 4 mm for both the first saw and the second saw.

The prices per volume unit of sawn timber used were relative with respect to center boards of quality T2. In Table 2 the relative prices are presented for each grade. The prices are representative for a typical Scandinavian sawmill producing strength graded timber.

Table 2: Price list with price differentiation between board grades. The prices are relative with the price for center boards grade T2 as reference.

Board type	Center boards					Side boards			Chips
Grade	T3	T2	T1	T0	Reject	A	B	C	-
Price/m^3	106	100	68	68	68	100	100	68	18

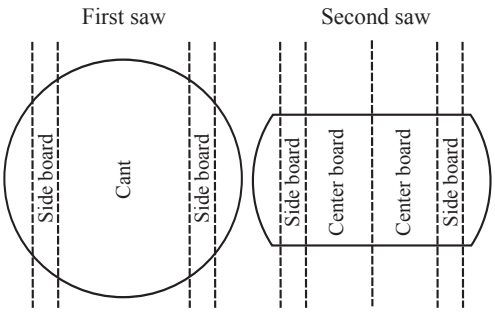

Figure 1: Cant sawing. The first sawing machine cuts the log into side boards and a cant. The cant is then rotated by 90 degrees and cut by the second sawing machine into side boards and center boards. Side boards are further processed by edging and trimming, while trimming is the only operation on center boards.

2.3 Simulation runs

Simulation of curve sawing of all logs in the ESSB was performed in each angle of rotation in the interval $[-90°, 90°]$, where the rotation angle of $0°$ corresponds to the horns down position. The term horns down refers to the log position in which a log with sweep (end-to-end curvature) is positioned so that the log ends are set down on the log carriage while the middle section of the log is off the carriage (Lundahl and Grönlund, 2010). This log positioning prior to sawing is common practice in the Scandinavian sawmills when applying curve sawing.

The outcome of the simulations are two functions: the value recovery, V, and the volume yield, Y, of the boards as functions of rotation angle. These are defined as

$$V = f(\theta), \qquad \theta \in [-90°, 90°], \tag{1}$$

$$Y = g(\theta), \qquad \theta \in [-90°, 90°], \tag{2}$$

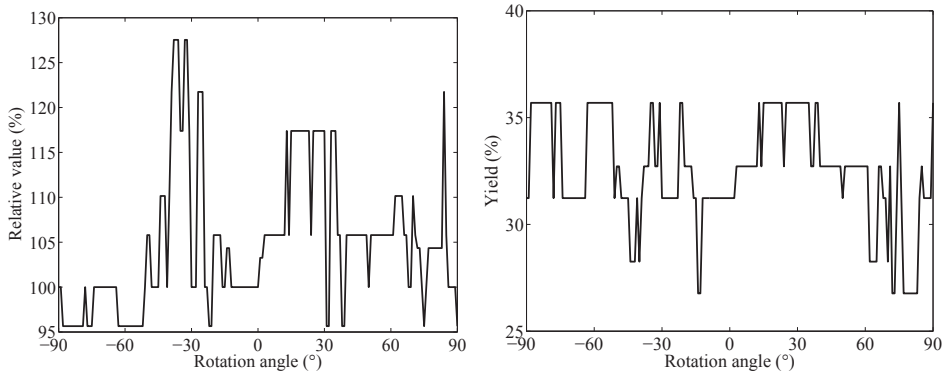

(a) (b)

Figure 2: The value function (a) and yield function (b) with respect to the strength graded center boards of a log. The value is relative to the value at the horns down position where the rotation angle of $0°$ *corresponds to the horns down position.*

where θ is the log rotation angle and $\theta = 0°$ is set as the horns down position. The value function, V, and yield function, Y, with respect to the strength graded center boards of one example log are shown in Figure 2. In the case where strength graded center boards, side boards and chips are considered, the value and yield functions look similar to the respective functions in Figure 2.

Let θ_i^{max} be the rotational position of log i relative to horns down that maximizes the value. If there are N logs, the average value recovery relative to horns down is

$$\overline{V}_{rel}^{max} = \frac{1}{N} \sum_{i=1}^{N} \frac{V_i(\theta_i^{max})}{V_i(0)}. \tag{3}$$

The average yield change for these choices of θ is calculated as

$$\overline{\Delta Y}_{V_{rel}^{max}} = \frac{1}{N} \sum_{i=1}^{N} (Y_i(\theta_i^{max}) - Y_i(0)). \tag{4}$$

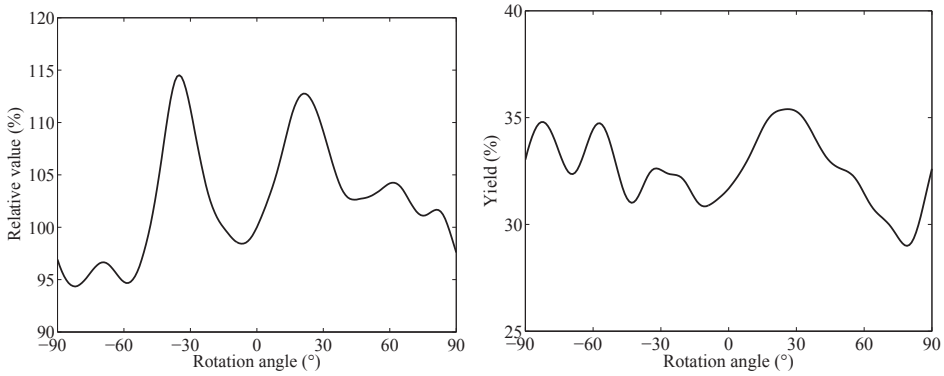

(a) (b)

Figure 3: The filtered value function (a) and the filtered yield function (b) obtained by applying a Gaussian filter to the value and yield function shown in Figure 3.2(a) and Figure 3.2(b). The Gaussian filter had a standard deviation of $\sigma = 5^{\circ}$ *and a window size of* $W_S = 29^{\circ}$*. The rotation angle of* 0° *corresponds to the horns down position.*

2.4 The effect of an error to the angle of rotation

A rotational error in a sawing machine is in this article assumed to be normally distributed $Z \in \mathcal{N}(\mu, \sigma))$, where μ is the expected value and σ is the standard deviation. In this study, the values of μ and σ were chosen to $\mu = 0^{\circ}$ and $\sigma = 5^{\circ}$. An estimate of the expected value and yield function of a sawing machine with a rotational error from a distribution $Z \in \mathcal{N}(0^{\circ}, 5^{\circ})$ was obtained using a Gaussian filter with $\sigma = 5^{\circ}$ and window size $W_S = 6\sigma - 1 = 6 \cdot 5 - 1 = 29^{\circ}$. Figure 3 shows an example of the effect of applying the Gaussian filter on the same value and yield functions as in Figure 2.

3 Results

3.1 Center boards

Table 3 shows the resulting average value increase and yield change for center boards if the value maximizing log rotation is chosen instead of the horns down position. The corresponding value for each SC is also

Table 3: Average value increase in percent and average yield change in percentage points when choosing the log rotational position that maximizes the value of the center boards in comparison with using the horns down position. Values both for an ideal rotation and with an applied rotational error, $Z \in \mathcal{N}(0°, 5°)$, are presented. N is the number of logs in corresponding SC used in the simulations.

SC	N	Average value increase (%)		Average yield change (pp)	
		Ideal	With error	Ideal	With error
1	86	8	4	0	0
2	64	9	5	0	0
3	63	9	5	0	0
4	46	9	5	0	0
5	55	10	6	0	0
6	37	11	6	0	0
7	35	15	7	1	0
8	68	14	8	0	0
9	47	17	9	0	0
10	57	11	7	1	0
11	43	11	7	1	1
12	36	14	7	0	0
13	22	12	6	1	0
14	18	13	7	0	1
Total	**677**	**11**	**6**	**0**	**0**

shown as well as the results when a rotational error from a distribution $Z \in \mathcal{N}(0°, 5°)$ is present.

For an ideal rotation, the average value increase for all SC is 11% compared to 6% with a rotational error. The corresponding change in volume yield is 0% in average both for an ideal rotation and with a rotational error. Histograms of center board value increase and yield change are shown in Figure 4. Figure 5 presents center board quality distribution when the center boards are value optimized. There is a shift of center board quality mainly from grade T1 at horns down position to grade T2 at the value optimized position.

3.2 Center boards, side boards and chips

Results when considering the total value of center boards, side boards and chips are shown in Table 4. The average value increase for an ideal rota-

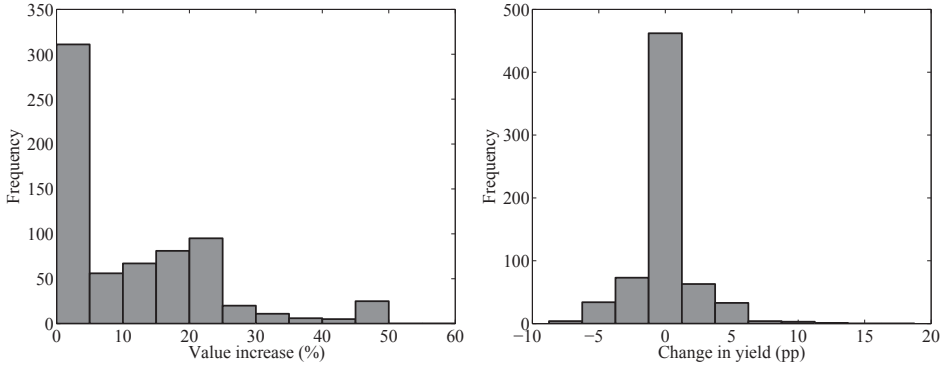

(a) (b)

Figure 4: Value increase in percent (a) and change in volume yield in percentage points (b) compared to the horns down position if using the log rotation that maximizes the value of the strength graded center boards.

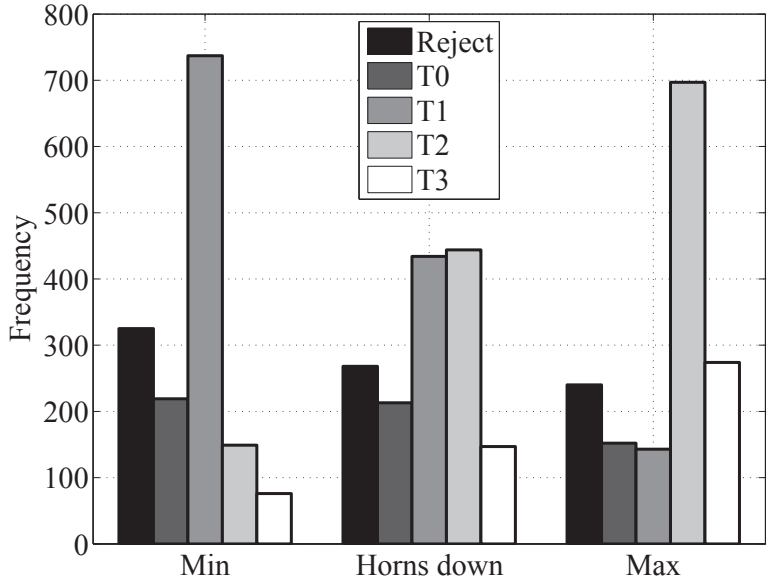

Figure 5: Sorting class of the strength graded center boards if the value of the center boards is considered when rotating the log. Min and max correspond to the rotational positions that result in the lowest and highest value recovery respectively.

Table 4: Average value increase in percent and average yield change in percentage points when choosing the log rotational position that maximizes the value of all products (center boards, side boards and chips) in reference to horns down position. Values both for an ideal and with an applied rotational error, $Z \in \mathcal{N}(0°, 5°)$, are presented. N is the number of logs in corresponding SC used in the simulations.

SC	N	Average value increase (%)		Average yield increase (pp)	
		Ideal	With error	Ideal	With error
1	86	9	5	2	1
2	64	9	5	2	1
3	63	8	4	1	0
4	46	7	4	0	0
5	55	15	8	5	3
6	37	13	7	3	1
7	35	12	6	3	1
8	68	15	8	3	2
9	47	14	7	2	1
10	57	11	6	3	1
11	43	9	5	2	1
12	36	13	6	4	2
13	22	9	5	2	1
14	18	10	6	2	2
Total	**677**	**11**	**6**	**2**	**1**

tion and with a rotational error applied is still 11% and 6% respectively. Change in volume yield is 2 pp in average for an ideal rotation and 1 pp in average with a rotational error present. Histograms of value increase and volume change are presented in Figure 6. The quality distribution of the center boards for this case is shown in Figure 7. As for the center boards, there is a shift of production mainly from center boards of quality T1 to T2.

4 Discussion

When considering all products (center boards, side boards, chips), the value increase was 11%. The quality of side boards depends of both knots and wane, where the latter in turn depends on log outer shape. For the obtained value increase of 11%, it would be interesting to know the impact

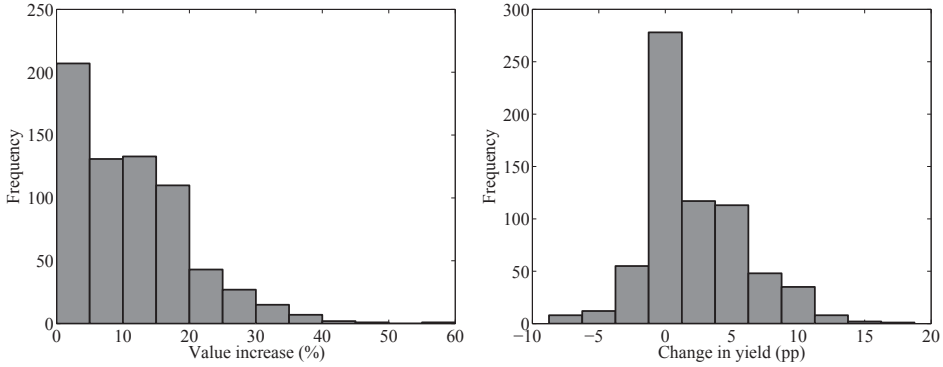

(a) (b)

Figure 6: Value increase in percent (a) and change in volume yield in percentage points (b) compared to the horns down position if using the log rotation that maximizes the total value of the strength graded center boards, appearance graded side boards and chips.

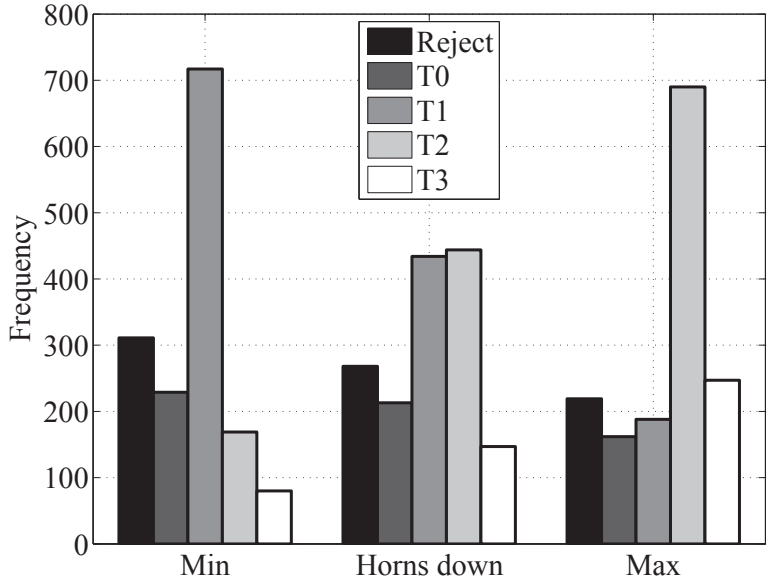

Figure 7: Sorting class of the strength graded center boards if the value of the center boards, side boards and chips is considered when rotating the log. Min and max correspond to the rotational positions that result in the lowest and highest value recovery respectively.

of knot structure and log outer shape respectively. This since log outer shape can be detected with a 3D scanner while knot structure information requires a CT scanner. To evaluate this, simulations of rotational optimization with respect to log outer shape are necessary. This has not been performed in this study. However, the value increase in the case when only considering center boards was also 11%. Since center boards originate from the center of logs, their quality is mainly governed by knots rather than wane. This indicates that information of the knot structure is important when optimizing log rotation with respect to the value of all products.

From the simulations, it is evident that a rotational error to the sawing machine reduces the average value increase, but that it is still profitable to rotate each log individually to obtain a higher value recovery. This means that a reduction in rotational error of the saw line results in a higher value recovery for a sawmill with a production strategy similar to the case in this study.

Berglund et al. (2013) simulated rotational optimization of the ESSB with quality grading entirely according to Nordic timber grading rules (Anon, 1997). Comparing the value increases of Berglund et al. (2013) and this study shows that they are close to each other. There seems to exist a value increase for logs in the ESSB larger than 10% for rotational optimization when using information of knot structure and applying grading rules mainly focusing on knots.

Splay knots due to top ruptures have a large impact on strength sorting according to SS 230120. The simplification made in this study to exclude such knots introduces an error in the results. For logs with top ruptures, the value of all sawn products would be lower if information of the top ruptures would be included. This applies to both horns down and the optimal rotational position. It is reasonable to expect that the difference between these values would increase since the optimization process would take into account top ruptures while the horns down position is independent of top ruptures.

SS 230120 describes additional defects, such as annual ring width, splits and spiral grain. Including those defects when determining board quality would give a more accurate simulation of visual strength grading, although knots and wane are the defects with the highest impact. To describe annual ring width, splits and spiral grain requires data and models that

can be added to a simulation software. This was not available in this study.

An interesting study would be to increase the degrees of freedom in the sawing simulation. Including skew and spatial positioning of logs, in addition to rotational positioning, would likely increase the optimization potential. The processing time would, however, increase as well.

5 Conclusion

The main conclusions of this article are that

- If using a CT scanner to optimize log rotation with respect to the value of visually strength graded center boards, appearance graded side boards and chips, the average value increase for the logs in this case study was 11%.
- A normally distributed rotational error with expected value $\mu = 0^\circ$ and standard deviation $\sigma = 5^\circ$ reduced the average value increase to 6%.
- The average value increase for the strength graded center boards only was also 11% for an ideal rotation and 6% with a rotational error present.
- The main reason for the value increase is that the share of strength graded center boards in sorting classes T2 and T3 is increased, while the share of boards in class T1 is reduced.

References

Anon, 1997: *Nordic Timber: Grading rules for pine (Pinus sylvestris) and spruce (Picea Abies) sawn timber: Commercial grading based on evaluation of the four sides of sawn timber.* Föreningen svenska sågverksmän (FSS), Sweden.

Berggren, G., S. Grundberg, A. Grönlund, and J. Oja, 2000: Improved spruce timber utilisation (STUD). Tech. rep., Luleå University of Technology and AB Trätek. European shared cost research project within FAIR (DGXII/E2), contract no. FAIR-CT96-1915. Final report sub-task A 1.2. Database and non-destructive "Glass-log" measurements.

Berglund, A., O. Broman, A. Grönlund, and M. Fredriksson, 2013: Improved log rotation using information from a computed tomography scanner. *Computers and Electronics in Agriculture*, **90**, 152–158, doi: 10.1016/j.compag.2012.09.012.

Björklund, L. and B. Julin, 1998: *Value optimised cross-cutting and sawing of CT-scanned Scots pine stems.* Swedish University of Agriculture Sciences, Uppsala, Sweden.

Björklund, L. and L. Moberg, 1999: Modelling the inter-tree variation of knot properties for Pinus sylvestris in Sweden. *Studia forestalia Suecica*, **207**.

EN 14081-1, 2011: Timber structures - Strength graded structural timber with rectangular cross section - Part 1: General requirements. CEN, Brussels, Belgium.

EN 14081-2, 2010: Timber structures - Strength graded structural timber with rectangular cross section - Part 2: Machine grading; additional requirements for initial type testing. CEN, Brussels, Belgium.

EN 14081-3, 2012: Timber structures - Strength graded structural timber with rectangular cross section - Part 3: Machine grading; additional requirements for factory production control. CEN, Brussels, Belgium.

Giudiceandrea, F., E. Ursella, and E. Vicario, 2011: A high speed CT scanner for the sawmill industry. *17th International nondestructive testing and evaluation of wood symposium*, F. Divos, Ed., Sopron, Hungary.

Johansson, C., 2003: Grading of timber with respect to mechanical properties. *Timber engineering*, 23–43.

Johansson, E., D. Johansson, J. Skog, and M. Fredriksson, 2013: Automated knot detection for high speed computed tomography on *Pinus sylvestris* L. and *Picea abies* (L.) Karst. using ellipse fitting in concentric surfaces. *Computers and Electronics in Agriculture*, **96**, 238 – 245, doi:http://dx.doi.org/10.1016/j.compag.2013.06.003.

Lundahl, C.-G. and A. Grönlund, 2010: Increased yield in sawmills by applying alternate rotation and lateral positioning. *Forest Product Journal*, **60**, 331–338.

Nordmark, U., 2005: Value recovery and production control in the forestry-wood chain using simulation technique. Ph.D. thesis, Luleå University of Technology, Luleå, Sweden.

Oja, J., 2000: Evaluation of knot parameters measured automatically in CT-images of Norway spruce (*Picea abies* (L.) Karst.). *European Journal of Wood and Wood Products*, **58 (5)**, 375–379.

SS 230120, 2010: INSTA 142. Nordic visual strength grading rules for timber. Swedish Standards Institute, Stockholm, Sweden.

Todoroki, C. L. and E. Rönnqvist, 1999: Combined primary and secondary log breakdown optimisation. *The Journal of the Operational Research Society*, **50 (3)**, pp. 219–229.